Geological Quarterly, 2015, **59** (4): 700–717
DOI: http://dx.doi.org/10.7306/gq.1232

Monazite Th-U-total Pb geochronology and P-T thermodynamic modelling in a revision of the HP-HT metamorphic record in granulites from Stary Gierałtów (NE Orlica–Śnieżnik Dome, SW Poland)

Bartosz BUDZYŃ[1, *], Mirosław JASTRZĘBSKI[2], Gabriela A. KOZUB-BUDZYŃ[3] and Patrik KONEČNÝ[4]

[1] Institute of Geological Sciences, Polish Academy of Sciences, Research Centre in Kraków, Senacka 1, 31-002 Kraków, Poland

[2] Institute of Geological Sciences, Polish Academy of Sciences, Research Centre in Wrocław, Podwale 75, 50-449 Wrocław, Poland

[3] AGH University of Science and Technology, Faculty of Geology, Geophysics and Environmental Protection, al. A. Mickiewicza 30, 30-059 Krakow, Poland

[4] Geological Institute of Dionýz Štúr, Mlynská dolina 1, SK–81704 Bratislava, Slovak Republic

Budzyń, B., Jastrzębski, M., Kozub-Budzyń, G.A., Konečný, P., 2015. Monazite Th-U-total Pb geochronology and P-T thermodynamic modelling in a revision of the HP-HT metamorphic record in granulites from Stary Gierałtów (NE Orlica–Śnieżnik Dome, SW Poland). Geological Quarterly, **59** (4): 700–717, doi: 10.7306/gq.1232

Thermodynamic modelling, geothermometric calculations and monazite Th-U-total Pb dating via electron microprobe analysis were used to improve the pressure, temperature and timing constraints of the HP-HT metamorphic record in granulites from Stary Gierałtów (NE Orlica–Śnieżnik Dome, SW Poland). The new data constrained the P-T conditions to 20–22 kbar and ca. 900–920°C, followed by decompression to ca. 16–18 kbar in the felsic-to-intermediate granulites and 18–20 kbar and ca. 950–970°C in the mafic granulite. The latter conditions are considered to closely represent the peak temperatures experienced by these rocks. In the intermediate granulite, the matrix monazite and monazite inclusions in garnet and allanite yielded an age of 349 ± 2.5 Ma. A HP-HT metamorphic event with temperature conditions exceeding 900°C, which are greater than the closure temperatures of most geochronometers, must have disturbed and completely reset the isotopic systems, including the Th-U-Pb system in the monazite. Consequently, this resetting prevented us from constraining the age of potential earlier metamorphic events or the igneous protolith. The 349 ± 2.5 Ma age is interpreted as the timing of the late-stage HP-HT event and cooling below 900°C related to the initial exhumation of the granulites. A comparison of the new P-T-t constraints with previous data from the NE Orlica–Śnieżnik Dome indicates that the activation of the channels that exhumed the HP rocks to middle crustal depths most likely initiated at ca. 349 Ma, and that all of the metamorphic rocks in the Orlica–Śnieżnik Dome likely shared a common Variscan evolution after ca. 340 Ma.

Key words: monazite, Th-U-total Pb dating, thermodynamic modelling, granulite, Orlica–Śnieżnik Dome, Bohemian Massif.

INTRODUCTION

Felsic and mafic granulites from the Orlica–Śnieżnik Dome (OSD, NE Bohemian Massif; Fig. 1A) provide records of high-pressure and high-temperature (HP-HT) metamorphic stages and have attracted the attention of scientists for decades. These volumetrically small but geodynamically significant rocks represent the Variscan orogenic root (Fig. 1B) and document vertical ductile extrusion and subsequent lateral spreading, both related to the Variscan assembly of Saxothuringia and Brunovistulia during the Variscan orogeny (Fig. 1A; Štípská et al., 2004; Schulmann et al., 2008). Numerous previous studies performed on these rocks have included petrographic and geochemical descriptions (Kozłowski, 1965; Smulikowski, 1967, 1979; Smulikowski and Bakun-Czubarow, 1973; Kądziałko-Hofmokl et al., 2013), estimates of the metamorphic pressure and temperature (P-T) conditions (Smulikowski, 1979; Pouba et al., 1985), geothermobarometric calculations (Bakun-Czubarow, 1991a; Kryza et al., 1996; Štípská et al., 2004; Szczepański et al., 2008; Bröcker et al., 2010), geochronology (Brueckner et al., 1991; Klemd and Bröcker, 1999; Štípská et al., 2004; Lange et al., 2005; Anczkiewicz et al., 2007; Kusiak et al., 2008; Bröcker et al., 2010; Walczak, 2011) and structural reconstructions (e.g., Dumicz, 1993; Štípská et al., 2004). Despite this broad dataset that includes geochronology and geothermobarometry, there is still room for debate with regard to whether these rocks experienced ultrahigh pressure peak metamorphic conditions, the

* Corresponding author, e-mail: ndbudzyn@cyf-kr.edu.pl

Received: February 27, 2015; accepted: May 19, 2015; first published online: May 20, 2015

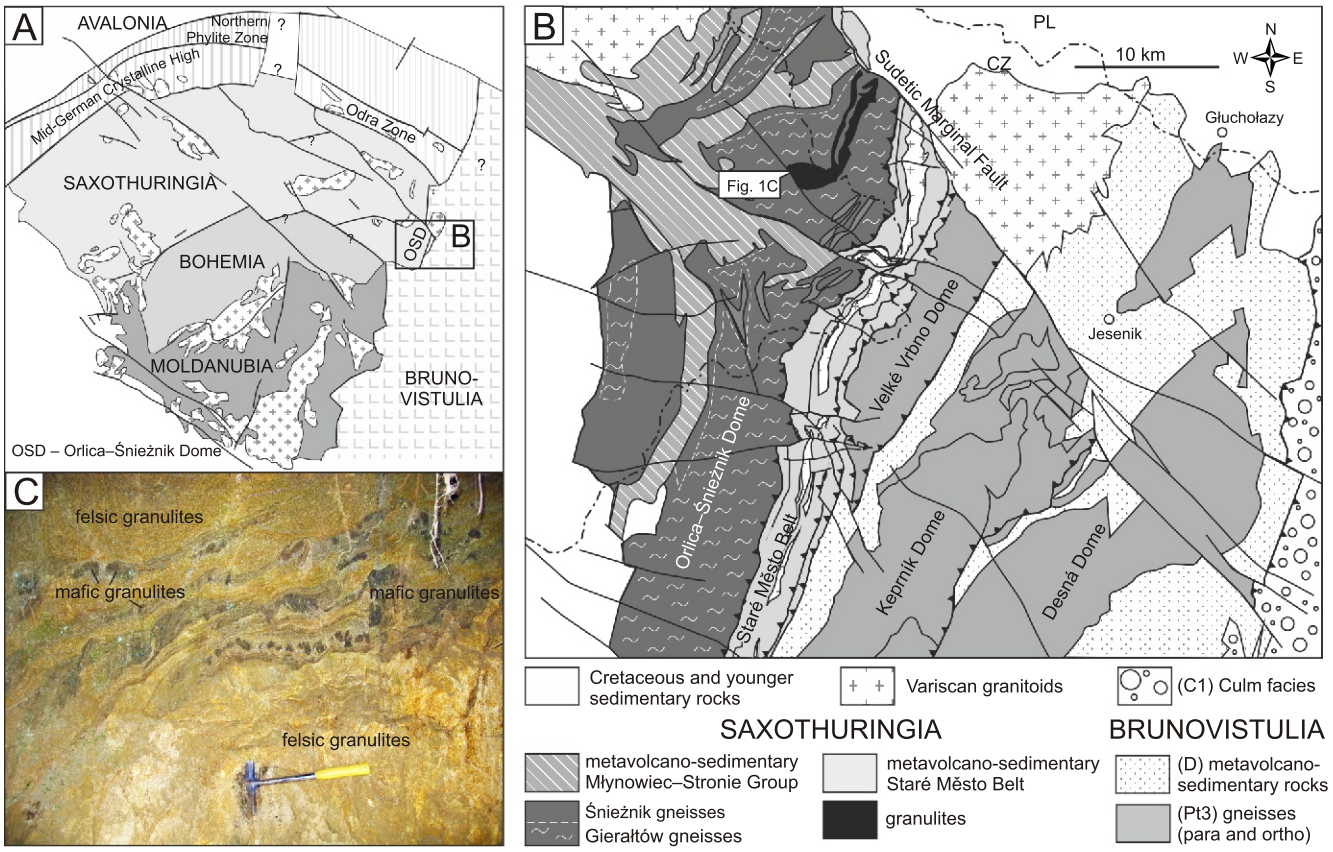

Fig. 1A – geological sketch showing the location of the Orlica–Śnieżnik Dome on a map of the Central European terranes (modified after Franke and Żelaźniewicz, 2000); B – location of the granulite body on a simplified geological map (modified after Sawicki, 1995; Schulmann and Gayer, 2000; Don et al., 2003); C – the sampled outcrop of granulites in the village of Stary Gierałtów at 50°18'30.2"N, 16°56'02.5"E

timing and duration of this ultra HP-HT metamorphic stage (dated to between ca. 337 and 382 Ma; Štípská et al., 2004; Lange et al., 2005; Anczkiewicz et al., 2007; Bröcker et al., 2010), and the suggested age record of the amphibolite-facies overprint (347 ± 13 Ma; Kusiak et al., 2008). Linking these distinct dates to metamorphic episodes along the P-T path recorded by the granulites is required to better understand the subduction and/or exhumation events related to the Variscan development of the Saxothuringia/Brunovistulia terrane boundary.

In this paper, we contribute to the ongoing discussion on the timing, P-T conditions and geodynamic significance of an HP-HT event recorded by the granulites by constraining the Th-U-total Pb age of monazite (via *in situ* analysis) and thermodynamic modelling. Together, these methods link the absolute age with specified P-T conditions. Three samples, representing felsic, intermediate and mafic granulites from the NE portion of the OSD (Fig. 1B, C), were used in a P-T pseudosection calculation to provide new insights into the conditions of both peak metamorphism and the decompression history. Conventional garnet-pyroxene geothermometry was also applied to the clinopyroxene-bearing intermediate and mafic granulites. Several samples representing all OSD granulite types were also examined under high-contrast backscattered electron (BSE) imaging in an electron microprobe to verify the presence of monazite. One thin section of the intermediate granulite was suitable for monazite geochronology and was selected for this study to verify the Th-U-total Pb age record. The application of geochronological *in situ* analysis, such as electron microprobe analyses, provides an opportunity to link dates from internal domains of monazite with the textural context to constrain the timing of particular geological processes (Williams and Jercinovic, 2002; Williams et al., 2007). Applying this new approach to the P-T-t record of the granulites improves our knowledge of the geodynamic development of the Orlica–Śnieżnik Dome in the frame of the colliding terranes during formation of the Variscan Orogen.

GEOLOGICAL SETTING AND PREVIOUS STUDIES

The Orlica–Śnieżnik Dome is located in the NE Bohemian Massif at the boundaries of the Saxothuringian, Moldanubian and Tepla-Barrandian terranes (Matte et al., 1990; Cymerman et al., 1997; Franke and Żelaźniewicz, 2000; Fig. 1A). In the east, the OSD borders the structurally lower Staré Město Belt and Brunovistulian (Brunia) Terrane (e.g., Schulmann and Gayer, 2000; Don et al., 2003; Mazur et al., 2006; Jastrzębski et al., 2015b; Fig. 1B). The OSD mainly consists of metavolcano-sedimentary rocks and gneisses that are traditionally subdivided into Śnieżnik augen orthogneisses and fine-grained, often migmatitic Gierałtów gneisses (Don et al., 1990; Redlińska-Marczyńska and Żelaźniewicz, 2011), which encompass subordinate bodies of (ultra?) high-pressure granulites and eclogites (e.g., Don et al., 1990; Fig. 1B). In the OSD, the felsic, intermediate and mafic granulites form an elongated belt that is 9 km long and up to 2 km wide within the migmatitic gneisses in the Góry Złote Mts. (Rychleby Mts. in the Czech

geographic nomenclature) near the northeastern margin of the OSD (Don et al., 2003; Fig. 1B). The felsic granulites are mainly composed of plagioclase, K-feldspar, quartz, garnet, biotite, kyanite and rare omphacite with accessory rutile, ilmenite, apatite, monazite and zircon. Thin boudinaged intercalations of more mafic varieties occur within the felsic granulites (Fig. 1C). The mafic granulites contain greater amounts of garnet and omphacite and lower quantities of quartz and plagioclase (Kozłowski, 1965; Smulikowski and Bakun-Czubarow, 1973).

The maximum pressures of metamorphism (exceeding 28 kbar) were estimated from an omphacite granulite based on the presence of quartz pseudomorphs after coesite (Bakun-Czubarow, 1991b, 1992). The pressure-temperature conditions of a maximum metamorphic stage recorded by an intermediate pyroxene-bearing granulite were determined using ternary feldspar thermometry, garnet-pyroxene thermometry and garnet-Al_2SiO_5-plagioclase-quartz (GASP) barometry. The P-T conditions exceeded 22 kbar (possibly ca. 30 kbar) and 900°C, with a retrogression to 22–25 kbar and 800–900°C recorded in the rims (Kryza et al., 1996). A later study also used ternary feldspar thermometry, garnet-clinopyroxene thermometry, GASP geobarometry and plagioclase-clinopyroxene-garnet-quartz (GADS) geobarometry in mafic granulites and eclogites and reported metamorphic conditions of 800–1000°C and 21–28 kbar (Klemd and Bröcker, 1999). The decreasing jadeite content in the omphacite rims indicated retrogression at 8–12 kbar and 500–740°C (Klemd and Bröcker, 1999). Štípská et al. (2004) reported that the granulites from the Góry Złote Mts. experienced pressure conditions up to 18–19 kbar at ca. 900°C and subsequent amphibolite facies overprint at 740°C and 8–10 kbar. However, Szczepański et al. (2008) documented a pressure peak estimated at 30 kbar and 700°C, followed by a temperature peak at 930°C and 27 kbar. Ti-in-zircon thermometry estimated metamorphic temperatures of ca. 885°C in a felsic granulite (Bröcker et al., 2010).

Several studies applied garnet, zircon and monazite dating to constrain the timing of (U)HP-HT metamorphic events in the granulites. The Sm-Nd dating of garnet-whole rock (Grt-WR) in a mafic granulite from Stary Gierałtów yielded ages of 341±10 Ma and 343 ± 11 Ma (Klemd and Bröcker, 1999), which are within the error of the Sm-Nd 352 ± 4 Ma age based on a garnet-clinopyroxene-whole rock (Grt-Cpx-WR) isochron from an eclogite from Stary Gierałtów (Brueckner et al., 1991). The Lu-Hf garnet dating of felsic and mafic granulites from Červený Důl (the Rychleby Mts., Czech Republic) provided ages of 357 ± 10 Ma (Grt-Cpx-WR, mafic granulite), 351 ± 10 Ma (Grt-WR, mafic granulite) and 337 ± 4 Ma (Grt-WR, felsic granulite), interpreted as the upper and lower time limits of UHP to HP metamorphism (Lange et al., 2005). Walczak (2011) obtained similar Lu-Hf garnet ages of 348.3 ± 2.0 Ma and 346.9 ± 1.2 Ma for garnet in felsic granulite samples and 343.2 ± 1.6 Ma in mafic granulite samples from Stary Gierałtów. The Sm-Nd dating of garnet from the same three sets of samples yielded ages of 332.4 ± 5.2 Ma, 337.6 ± 2.3 Ma and 336.9 ± 6.0 Ma, respectively (Walczak, 2011). Significantly older Lu-Hf ages for garnet growth during prograde UHP metamorphism were constrained to 386.6 ± 4.9 Ma in felsic granulite samples and 373.8 ± 4.0 Ma in mafic granulite samples (Anczkiewicz et al., 2007). The same study reported younger Sm-Nd garnet ages of 340.1 ± 4.1 Ma in mafic granulite samples and 320.5 ± 3.0 Ma in felsic granulite samples (Anczkiewicz et al., 2007).

In the mafic granulite, zircon crystallisation from the melt was constrained to 360–369 Ma using $^{207}Pb/^{206}Pb$ dating (Klemd and Bröcker, 1999). SHRIMP evaporation zircon dating yielded mean U-Pb and Pb-Pb ages of 342 ± 5 Ma and 341.4 ± 0.7 Ma, respectively, which were interpreted as the timing of the peak metamorphism concurrent with the onset of the vertical extrusion of the granulites (Štípská et al., 2004). The SHRIMP and LA-ICP-MS U-Pb ages of the overprint that resulted in the growth of metamorphic zircon and alterations in the zircon originating from the protolith of the eclogites and granulites were constrained to 350–330 Ma. These ages are associated with (U)HP rocks related to late-stage eclogite-facies metamorphism but not to middle crustal metamorphic processes (Bröcker et al., 2010). Walczak (2011) reported a similar 342.2 ± 5 Ma U-Pb age for the zircon overgrowths in felsic granulite. Comparable $^{206}Pb/^{238}U$ ages were observed in spherical zircons from mafic granulite (340.2 ± 1.2 Ma and 341.1 ± 1.3 Ma) and from felsic granulite (338.1 ± 1.3 Ma) (Lange et al., 2005). A significantly younger zircon $^{206}Pb/^{238}U$ age of 326 ± 1.5 Ma was observed in felsic granulite from the same study and interpreted as being related to a late stage of the cooling path from amphibolite to greenschist facies (Lange et al., 2005). The older $^{206}Pb/^{238}U$ ages yielded by prismatic zircons should also be noted: 411.4 ± 1.5 Ma, 413.5 ± 1.6 Ma, and 359.3 ± 0.8 Ma in mafic granulite and 393 ± 2.8 Ma and 347 ± 1.4 Ma in felsic granulite (Lange et al., 2005).

Currently, only one study has included monazite Th-U-total Pb chronology. That study reported an average monazite age of 347 ± 13 Ma based on a wide range of single dates from 278 to 411 Ma (Kusiak et al., 2008). The authors related the monazite age to monazite growth during amphibolite-facies metamorphism post-dating a UHP metamorphic event.

MINERALOGY, THERMODYNAMIC MODELLING AND P-T CONSTRAINTS

SAMPLE SELECTION AND ANALYTICAL METHODS

For the P-T reconstructions of the OSD granulites, three mineralogically varied samples collected from an outcrop in the village of Stary Gierałtów (Fig. 1C; 50°18'30.2"N, 16°56'02.5"E) were selected. The samples are: (1) GS55-4, a felsic granulite; (2) Gr-pb, an intermediate granulite; and (3) GS55-1, a mafic granulite. The petrography and chemistry of all granulite types that crop out in Stary Gierałtów are well described in numerous previous works (Kozłowski, 1965; Smulikowski and Bakun-Czubarow, 1973; Bakun-Czubarow, 1991a, b; Kryza et al., 1996; Klemd and Bröcker, 1999). Therefore, the descriptions of the felsic, intermediate and mafic granulites selected for this study focus primarily on the mineral chemistry crucial for further P-T determinations.

Preliminary microstructural observations and mineral identification were performed using a *Cameca SX 100* electron microprobe at the Electron Microprobe Laboratory, University of Warsaw. Chemical analyses of silicates in carbon-coated thin sections were performed using a *JEOL SuperProbe JXA-8230* electron microprobe equipped with five wavelength-dispersive spectrometers in the Laboratory of Critical Elements AGH-KGHM at AGH University of Science and Technology (Kraków, Poland). The accelerating voltage was 15 kV, and the beam current was 20 nA. A 3–5 μm beam size was used for feldspars and micas, and a focused beam was used for garnets and pyroxenes. The peak and background counting times were 10 and 5 seconds, respectively, for all elements, except for Si, which received 20 and 10 seconds, respectively. Additionally allanite was analysed using a *Cameca SX 100* electron microprobe at the Department of Special Laboratories, Laboratory of Electron Microanalysis, Geological Institute of Dionýz

Štúr (Bratislava, Slovak Republic). The analytical conditions included the accelerating voltage 15 kV, the beam current 40 nA and 3 μm beam size. Results of the electron microprobe analyses of silicates are presented in Appendices 1–5*.

Thermodynamic modelling in the NCKFMASHTO (Na_2O-CaO-K_2O-FeO-MgO-Al_2O_3-SiO_2-H_2O-TiO_2-Fe_2O_3) system was performed using the *THERMOCALC* program, which contains the thermodynamic database of Holland and Powell (1998, dataset 55; November 2003 update). The P-T pseudosections were calculated in the P-T window ranging from 10 to 30 kbar and from 700 to 1000°C. Garnet, orthopyroxene, clinopyroxene, muscovite, biotite, plagioclase, K-feldspar, quartz, melt, ilmenite, kyanite, rutile and water were considered in the calculations. The activity-composition models used in the thermodynamic modelling were after Green et al. (2007) for clinopyroxene; White et al. (2007) for biotite, garnet and melt; Coggon and Holland (2002) for muscovite; Holland and Powell (2003) for K-feldspar and plagioclase; and White et al. (2000) for ilmenite. The whole-rock major element chemical compositions (Appendix 6), which were used to approximate the effective bulk compositions, were determined via lithium metaborate/tetraborate fusion with subsequent analysis by inductively coupled plasma mass spectrometry at Activation Laboratories, Ltd. (Actlabs, Canada).

The choice of the relevant bulk composition for the thermodynamic modelling of granulite-facies rocks presents many difficulties (see review in Kelsey and Hand, 2015). The most important issue is the estimation of the H_2O content because the stability of mineral assemblages depends greatly on this value. Open-system behaviour characterizes the granulite-facies conditions; however, certain features suggest low H_2O concentrations in the OSD granulites during at least the development of the granulite-facies mineral assemblages and subsequent retrogression. The lines of evidence for a low H_2O content include the relatively good preservation of the granulite-facies minerals (e.g., Kryza et al., 1996) and the small quantities of hydrous minerals (muscovite and biotite) in the studied rocks (usually <1% of the rock volume). Moreover, the whole-rock chemistry of all the studied samples reveals negative loss on ignition (LOI) values, which indicate increased mass during ignition due to the oxidation of FeO to Fe_2O_3. This observation indicates both low H_2O concentrations and the significant predominance of ferrous iron over ferric iron in the studied granulites. Previous geochemical studies on the Góry Złote granulites indicated variable proportions of Fe_2O_3 and FeO, with the occasional predominance of Fe_2O_3 (Kozłowski, 1965; Smulikowski and Bakun-Czubarow, 1973). However, the mineral composition of the studied rocks proves that ferric iron represents the less significant component. Based on the mineral composition and mass increase during ignition, the content of ferric iron in the pseudosection calculations was estimated to be 5% of the total iron and the content of H_2O was estimated to be 1 wt.%. Previous studies on the granulites from Stary Gierałtów indicate that significant high-temperature metamorphic conditions of 900–1000°C should produce some quantity of melt (Kryza et al., 1996), and melt inclusions in garnet were recently reported (Ferrero et al., 2015). All of these observations were considered in order to estimate the Fe_2O_3 and H_2O contents that make it possible to stabilize: (1) the observed granulite-facies mineral assemblage in the most mineralogically varied sample Gr-pb (composed of garnet, clinopyroxene, K-feldspar, plagioclase, rutile, quartz, and muscovite, which additionally was stable in the presence of a liquid (melt)) and (2) a retrograde mineral assemblage that includes biotite and ilmenite in the same sample. To constrain the P-T conditions, the compositional isopleths were calculated for the major minerals composing the granulite types studied.

Additionally, the recent calibration of the garnet-pyroxene geothermometer by Nakamura (2009) was applied to the pyroxene-bearing intermediate and mafic granulites (Gr-pb and GS55-1). The calibration was formulated based on the analysis of a large experimental dataset, Nakamura (2009) shows that previous calibrations overestimated the metamorphic temperatures by 100–200°C for temperatures <1300°C, particularly in high-Ca garnets (XCa = 0.3–0.5). The new calibration also constrains the temperatures to 20–100°C lower than previous estimates based on natural eclogites. The recalibration of the method is intended for temperature conditions of 800–1820°C with a 74°C 1-sigma standard deviation (Nakamura, 2009). Therefore, the application of this method provides an improved insight into the temperature conditions of the granulite-facies metamorphism in the OSD.

The mineral abbreviations used in this paper are after Whitney and Evans (2010). The other abbreviations include the following (in %): Grs (Grt) = Ca/(Mn+Fe^{2+}+Mg+Ca) x 100; Alm (Grt) = Fe/(Mn+Fe^{2+}+Mg+Ca) x 100; Prp (Grt) = Mg/(Mn+Fe^{2+}+Mg+Ca) x 100; Sps (Grt) = Mn/(Mn+Fe^{2+}+Mg+Ca) x 100; XFe (Grt, Cpx, Bt) = Fe^{2+}/(Fe^{2+}+Mg) x 100; XCa (Grt) = Ca/(Fe^{2+}+Mg+Ca) x 100; An (Pl, Kfs) = Ca/(Ca+Na+K) x 100; Ab (Pl, Kfs) = Na/(Ca+Na+K) x 100; Or (Pl, Kfs) = K/(Ca+Na+K) x 100; and XNa (Cpx) = Na/(Na+Ca) x 100.

FELSIC GRANULITE – SAMPLE GS55-4

Petrography and mineral chemistry. The felsic granulite (GS55-4) is primarily composed of plagioclase ($Ab_{88–89}An_{10–11}Or_{1–2}$), quartz, K-feldspar and garnet (Fig. 2A, B). with minor amounts of biotite. Accessory phases include rutile, zircon, titanite, ilmenite and apatite. The felsic granulite shows no textural orientation. The garnet profiles from core to rim show zonation with a slight decrease in grossular (Grs from 32 to 28) and XFe (from 86 to 81), a simultaneous increase in pyrope (Prp from 9 to13), and relatively constant Fe and Mn concentrations throughout the garnet grains (Alm = 56–58, Sps 1; Fig. 3A, B).

Thermodynamic modelling and P-T evolution. The stability of plagioclase and K-feldspar constrain the maximum pressure of the felsic granulite sample (Fig. 4B) to ca. 17 kbar at 700°C and 25 kbar at 1000°C. The P-T pseudosection calculated for the bulk composition of the felsic granulite shows that the observed mineral assemblage represents the quinivariant field Grt-Kfs-Pl-Qz-Rt-Liq (Fig. 2A, B). This assemblage is stable above 800°C and 16 kbar (Fig. 4A).

The garnet and plagioclase compositional isopleths, which represent their measured chemical composition, shows that these variables are mainly pressure dependent (Fig. 5C); therefore, the temperatures cannot be estimated easily. The An(Pl) isopleths suggest that plagioclase formation occurred at conditions at which kyanite and/or muscovite were stable, but these two phases have been not observed. Therefore, the compositional isopleths of plagioclase probably cannot be used to derive the exact P-T conditions of the development of the mineral assemblage in this sample. There is a weak correlation between the XFe and XCa zoning in garnet and the trends of these isopleths in the P-T stability diagram. The zoning in the XFe in garnet and XCa suggests that the rock recorded a slight temperature increase and/or pressure decrease below ca. 16 kbar during garnet growth (Fig. 5C).

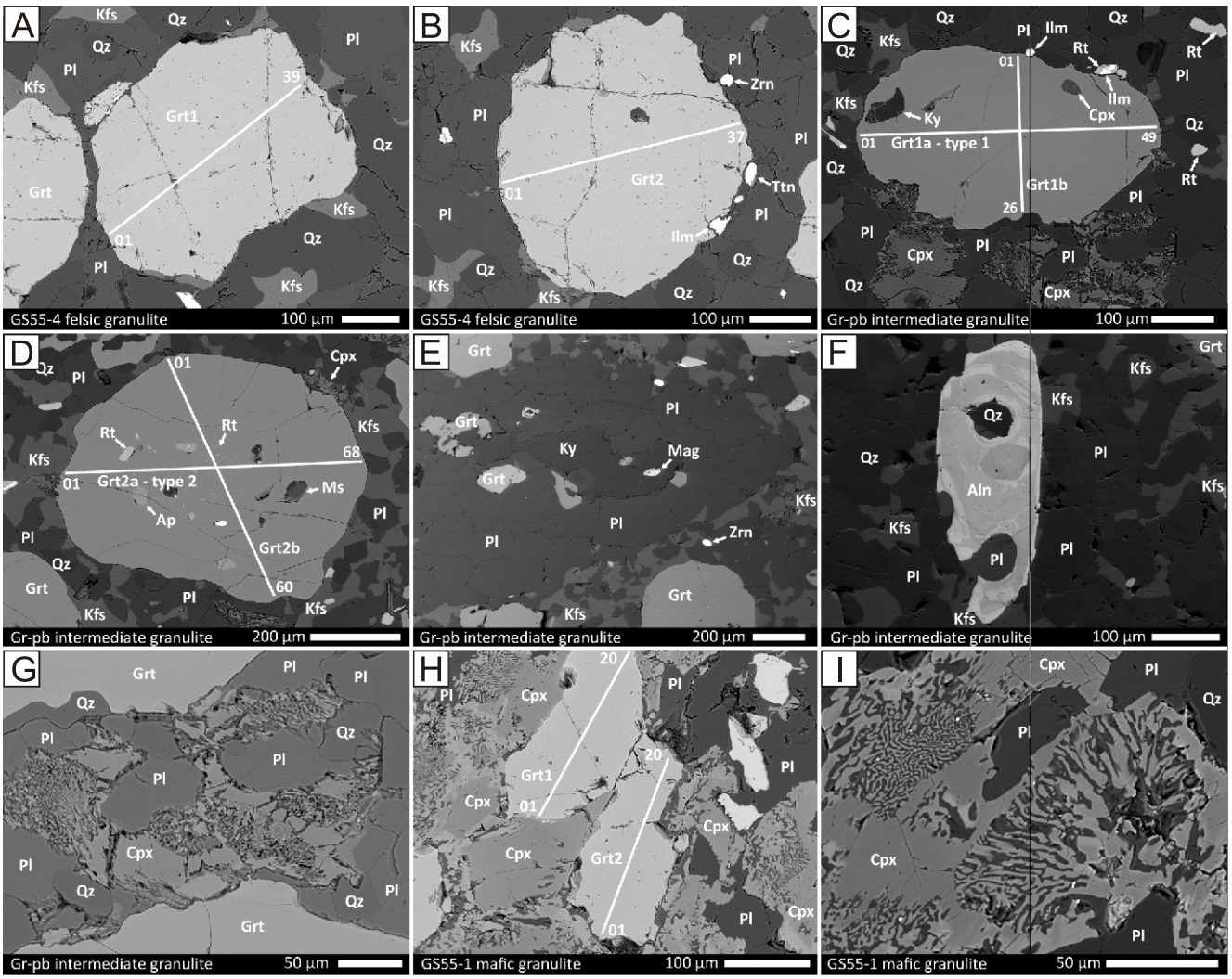

Fig. 2. Backscattered electron (BSE) images presenting the textural relationships of the minerals in the felsic (A, B), intermediate (C–G) and mafic (H, I) granulites

Analytical profiles of garnets are presented in Figure 3; Aln – allanite, Ap – apatite, Cpx – clinopyroxene, Grt – garnet, Ilm – ilmenite, Kfs – K-feldspar, Ky – kyanite, Mag – magnetite, Ms – muscovite, Pl – plagioclase, Qz – quartz, Rt – rutile, Ttn – sphene, Zrn – zircon

INTERMEDIATE GRANULITE – SAMPLE GR-PB

Petrography and mineral chemistry. The intermediate granulite (sample Gr-pb) is composed of garnet, plagioclase ($Ab_{84–89}An_{12–13}Or_{2–3}$; Appendix 1), K-feldspar, and quartz, with minor clinopyroxene, biotite, kyanite, rutile and ilmenite (Fig. 2C–G). Monazite, zircon, allanite and apatite are present as accessory phases. The granulite shows rough preferred orientation of elongated grains of garnet, rutile, plagioclase, kyanite, clinopyroxene and biotite. Biotite flakes are present in the rock matrix, mainly occurring around garnet blasts. The type 1-zoned garnet reflects a zonation with decreasing grossular content and increasing pyrope content from core to rim, accompanied by a slight decrease in the almandine composition (Alm from 52 to 49, Prp from 18 to 23, Grs from 30 to 26, Sps 1 and XFe from 74 to 69 from core to rim; Figs. 2C and 3C, D). The second type of garnet grain contains higher Mg and lower Ca concentrations and exhibits a profile with increasing grossular and decreasing pyrope and almandine concentrations towards the rim (Alm from 54 to 48, Prp from 30 to 27, Grs from 17 to 23, and Sps 1 and XFe close to 65 from core to rim; Figs. 2D and 3E, F). Rare muscovite flakes (3.18–3.22 Si p.f.u) were only recognized as inclusions in both types of garnet (Fig. 2D). whereas kyanite grains primarily occur as inclusions in garnet of type 1 and plagioclase blasts (Fig. 2C, E). The type 1 garnet also contains inclusions of clinopyroxene ($XNa_{49–51}$) (Fig. 2C). apatite, monazite, and K-feldspar. Matrix clinopyroxene with an omphacitic composition ($XNa_{24–37}$) is surrounded by thin symplectitic intergrowths of plagioclase and clinopyroxene with low Na concentrations ($XNa_{6–10}$). The symplectitic clinopyroxene is partially altered and replaced by submicroscopic-scale amphibole (Appendix 4). Allanite forms anhedral, zoned grains up to ca. 440 m long and ca. 150 m wide (Fig. 2F; Appendix 5). The concentric zoning suggests an origin related to a magmatic protolith. The allanite crystals contain inclusions of perthitic feldspar and quartz, which most likely formed under granulite-facies conditions.

Thermodynamic modelling and P-T evolution. The P-T pseudosection calculated based on the estimated bulk composition shows relatively good agreement with the observed changes in the mineral assemblages (Figs. 2C, D and 5A). The Grt-type 1 core assemblage that includes kyanite, muscovite,

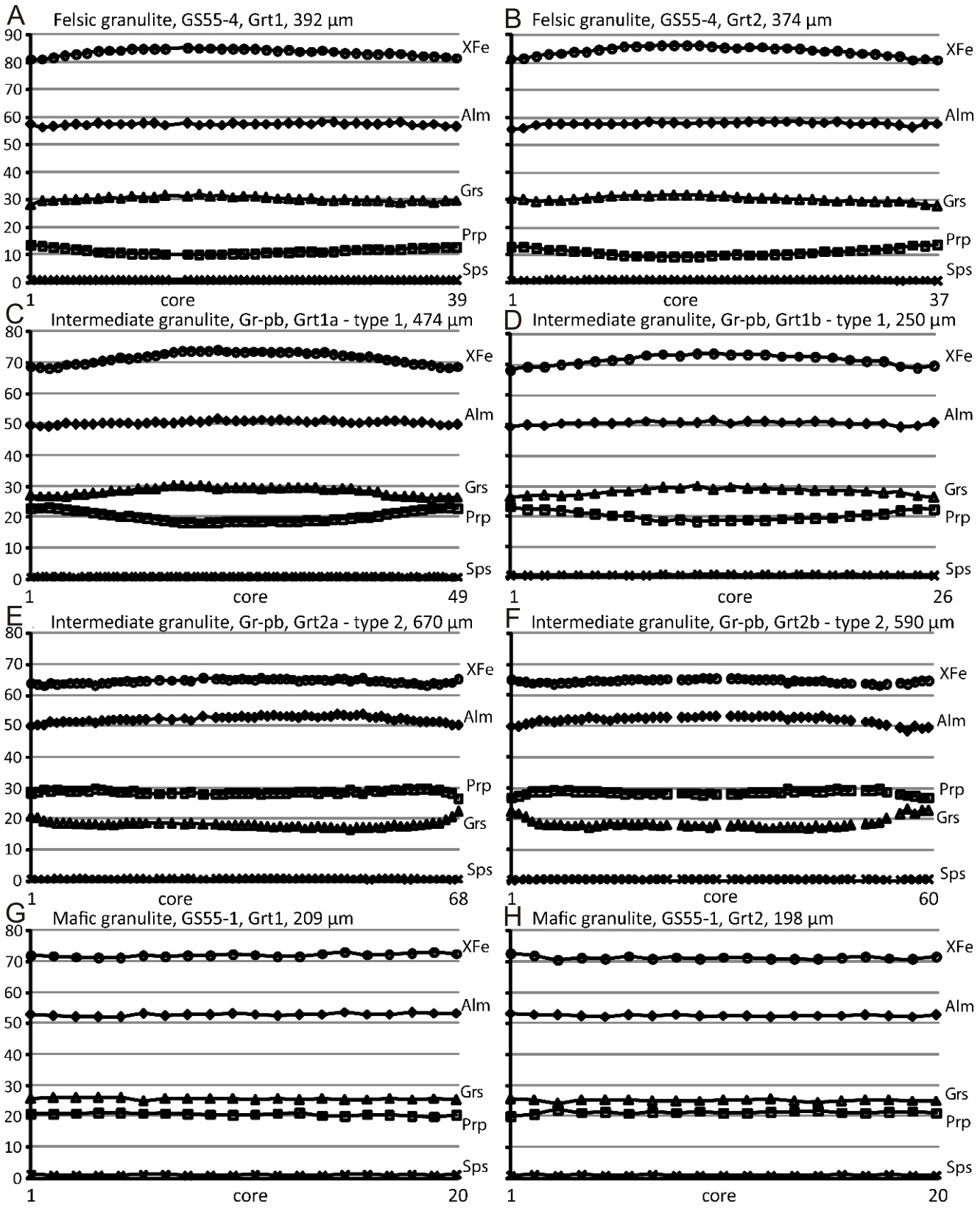

Fig. 3. Garnet profiles of the Alm, Prp, Grs, Sps and XFe of the grains presented in Figure 2

The electron microprobe results are presented in Appendix 3

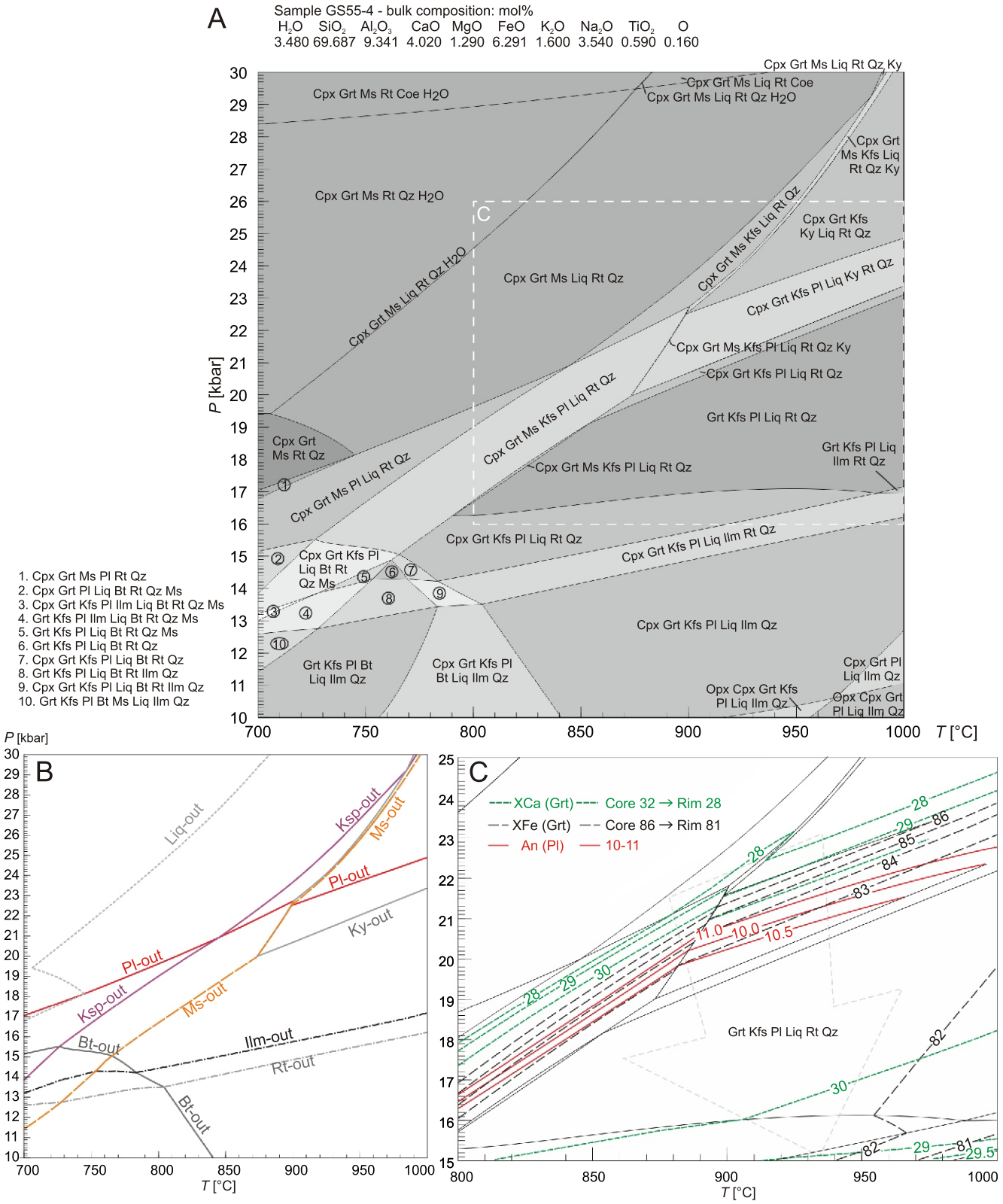

Fig. 4A – P-T pseudosection calculated for the felsic granulite rock composition (sample GS55-4); B – calculated stability of the rock-forming minerals; C – enlarged portion of the P-T pseudosection showing the calculated compositional isopleths compared to the measured chemical composition of the garnet and plagioclase

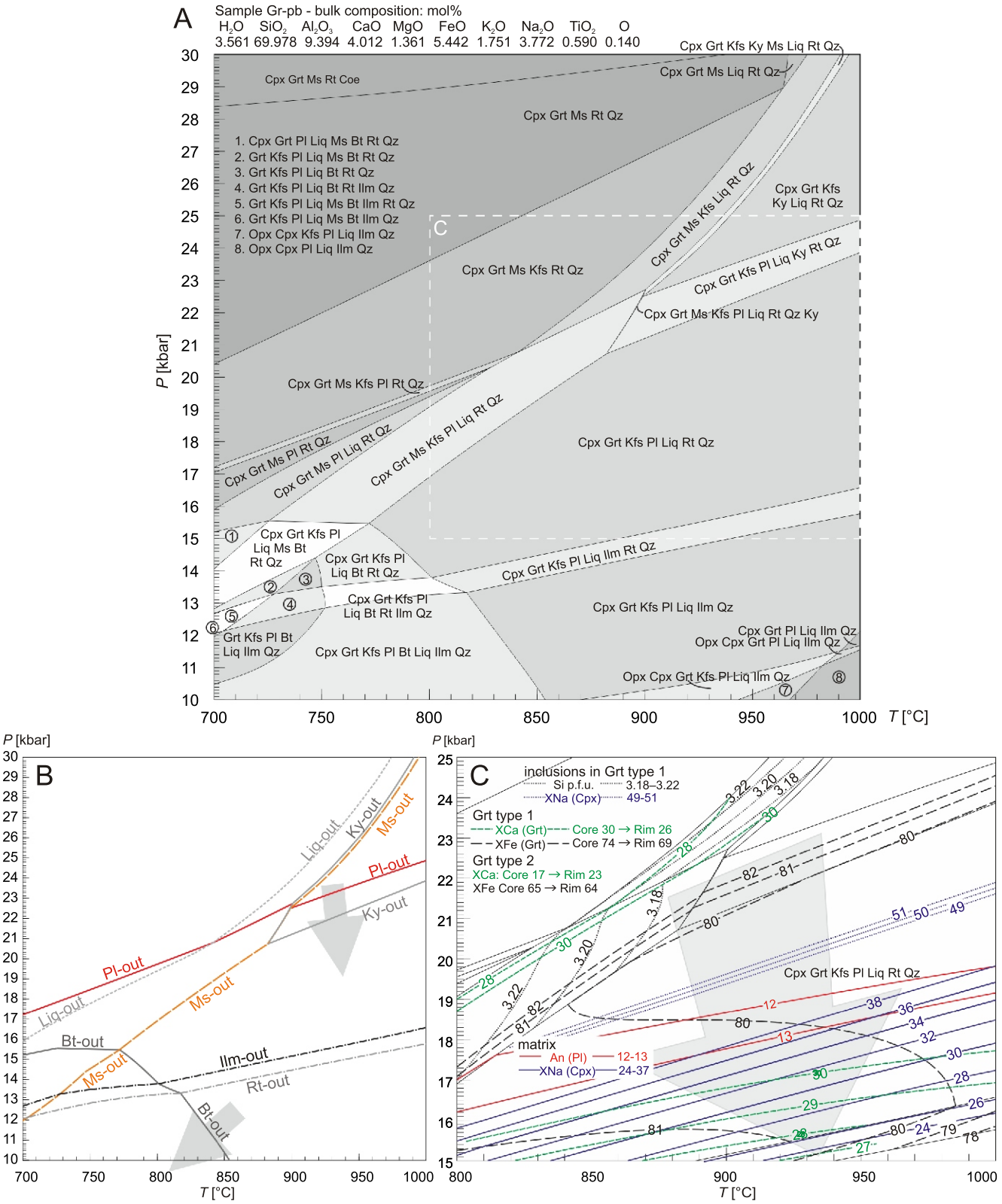

Fig. 5A – P-T pseudosection calculated for the intermediate granulite rock composition (sample Gr-pb); B – calculated stability of the rock-forming minerals with the possible P-T path derived from the succession of assemblages; C – enlarged portion of the P-T pseudosection showing the calculated compositional isopleths compared to the measured chemical composition of the garnet, plagioclase and clinopyroxene in the peak temperature mineral assemblage

clinopyroxene, quartz and rutile (Fig. 2C) is stable above 900°C and 22.5 kbar (Fig. 5A). The assemblage that also includes plagioclase can be related to the very narrow three-variant field Cpx-Grt-Ms-Kfs-Pl-Ky-Liq-Rt-Qz, which is stable between 20.5 and 22.5 kbar and between 890 and 900°C. The disappearance of kyanite and muscovite documents a pressure decrease and a transition to the quinivariant field Cpx-Grt-Kfs-Pl-Liq-Rt-Qz (Fig. 5B). Further decompression is evidenced by the appearance of ilmenite and biotite and the breakdown of primary omphacite to secondary symplectic clinopyroxene and plagioclase (Fig. 5C). The submicroscopic amphiboles noted within these symplectites could evidence the progressive uplift and cooling to amphibolite facies conditions.

The Cpx-Grt-Kfs-Pl-Liq-Rt-Qz stability field and adjacent P-T regions were contoured with isopleths of Si p.f.u in the muscovite, XNa (Cpx), XCa (Pl), XCa (Grt) and XFe (Grt) contents. The P-T conditions of the assemblages containing kyanite, muscovite, clinopyroxene, and quartz observed within type 1 garnet are further constrained by the calculated isopleths (Si p.f.u. in muscovite and XNa in clinopyroxene) in Figure 5C. The decreasing Na content in the clinopyroxenes (Fig. 2C) indicates the decompression path during growth of type 1 garnet. The stability diagram shows that small clinopyroxene grains included in type 1 garnet represent the P-T space ranging from 18 kbar and 850°C to 24 kbar and 1000°C. The predominant clinopyroxene blasts that occur in the matrix represent pressure conditions of ca. 2 kbar lower (Fig. 5C). Within the Cpx-Grt-Kfs-Pl-Liq-Rt-Qz stability field, the decompression to ca. 16–18 kbar is also documented by the decreasing zoning of type 1 Grt in X(Ca), X(Ca) Grt, XCa (Pl) and X(Na) Cpx indicate that the main granulite facies conditions assemblage developed within a P-T space between 900–970°C and 16–19 kbar. It is important to note that the XFe values of the two types of garnets are not predicted by the pseudosection. One explanation is the overestimation of the Fe^{2+} content with respect to the Fe^{3+} content in the bulk composition used in the calculations. A second explanation is that the XFe isopleths might not be predicted by the calculations because the chemical analysis may not represent the chemical composition of the thin section, or the rock was not equilibrated at a thin section scale. Moreover, it is not possible to constrain the P-T sector for the development of the garnet with increasing grossular content (type 2 garnet) because the correlation of the measured chemistry of type 2 garnet does not correspond to the isopleths in the pseudosection. However, the chemical zonation suggests that this garnet could have grown during the early progressive metamorphic path.

The thermodynamic modelling in this sample indicates good correlation of the stability diagram with the observed succession of assemblages; however, the chemistry of the minerals only partially fits these fields. The observed mineral succession and thermodynamic modelling indicate the decompression path from ca. 20–22 kbar to 16–18 kbar, but the temperature constraints on this event remain less defined. The calculated P-T pseudosection shows that the assemblage Cpx-Grt-Kfs-Pl-Bt-Liq-Ilm-Qz is stable under conditions up to 13 kbar and 850°C (Fig. 5). To shed more light on the temperature conditions of the granulite facies decompression, the garnet-pyroxene geothermometer by Nakamura (2009) was applied. The core of the type 1 garnet and clinopyroxene inclusion pair (Fig. 2C) yielded average temperatures of 885°C for pressure of 20 kbar (Table 1). A slightly higher average temperature of 899°C was obtained for the garnet rims and matrix clinopyroxene.

MAFIC GRANULITE – SAMPLE GS55-1

Petrography and mineral chemistry. The mafic granulite (GS55-1) contains significantly higher quantities of garnet and clinopyroxene than the felsic and intermediate granulites. Other minerals include plagioclase ($Ab_{84–87}An_{12–14}Or_{1–2}$), quartz, biotite and accessory rutile, ilmenite, zircon and apatite. In contrast to the more felsic varieties, the studied sample is free of K-feldspar. The garnet profiles show nearly homogeneous compositions of Alm = 51–54, Prp = 19–22, Grs = 24–26, Sps = 1 and XFe = 72–73 (Figs. 2H and 3G, H). Common clinopyroxene, represented by omphacite (XFe = 38–39 and XNa = 27–34). forms anhedral grains, which are also intergrown with garnet. Clinopyroxene also forms randomly oriented symplectites with plagioclase (Fig. 2H, I).

Thermodynamic modelling and P-T evolution. The thermodynamic modelling reveals good agreement with the observed relatively simple mineralogy that could represent the six-variant field Grt-Pl-Cpx-Rt-Liq-Qz (Fig. 6A, B). The relatively flat compositional profiles of the garnet and pyroxenes indicate diffusional homogenization related to the peak temperature conditions. The intersection of the compositional isopleths of XFe (Cpx), XNa (Cpx), and XFe (Grt) constrains the P-T of this episode to conditions of 18–20 kbar and 940–970°C (Fig. 6C). The X(Ca) Grt isopleths do not intersect with those mentioned above, suggesting the that the homogenization event in these rocks might occur at pressures 1–2 kbar lower. The presence of Cpx symplectites, ilmenite and biotite indicates decompression to conditions less than 14 kbar and 850°C (Fig. 6B).

The garnet-pyroxene geothermometer (Nakamura, 2009) applied to three garnet-clinopyroxene pairs from the mafic granulite yielded temperatures of 959°C for 20 kbar, ca. 60–75°C higher than those calculated for the Gr-pb sample, in accordance with the P-T pseudosection calculations.

Th-U-total Pb DATING OF MONAZITE

ANALYTICAL METHODS

The chemical analyses of monazite in sample Gr-pb for Th-U-total Pb dating were conducted using a *Cameca SX 100* electron microprobe, equipped with four wavelength-dispersive spectrometers (WDS) at the Department of Special Laboratories, Laboratory of Electron Microanalysis, Geological Institute of Dionýz Štúr (Bratislava, Slovak Republic). The electron microprobe, which was equipped with large diffraction crystals, performs high-precision and high-accuracy trace element analysis, which is crucial in dating monazite. The monazite in a carbon-coated thin section was analysed under conditions of a 15kV accelerating voltage, 180 nA beam current and 3 μm beam size. The following natural and synthetic standards and corresponding spectral lines were used for the analyses: apatite (P K), $PbCO_3$ (Pb M), ThO_2 (Th M), UO_2 (U M), YPO_4 (Y L), $LaPO_4$ (La L), $CePO_4$(Ce L), $PrPO_4$ (Pr L), $NdPO_4$ (Nd L), $SmPO_4$ (Sm L), $EuPO_4$ (Eu L), $GdPO_4$ (Gd L), $TbPO_4$ (Tb L), $DyPO_4$ (Dy L), $HoPO_4$ (Ho L), $ErPO_4$ (Er L), $TmPO_4$ (Tm L), $YbPO_4$ (Yb L), $LuPO_4$ (Lu L), fayalite (Fe K), barite (S K), wollastonite (Ca K , Si K), $SrTiO_3$ (Sr L), Al_2O_3 (Al K), and GaAs (As L). The counting times (in seconds) for the peak/background were as follows: P 10/10, Pb 300/150, Th 35/17.5, U 80/80, Y 40/20, La 5/5, Ce 5/5, Pr 15/15, Nd 5/5, Sm 5/5, Eu 25/25, Gd 10/10, Tb 7/7, Dy 35/35, Ho 30/30, Er 50/50, Tm 15/15, Yb 15/15, Lu 100/100, Fe 5/5, S 10/10, Ca 10/10, Sr 20/20, Al 10/10, Si 10/10, and As 120/120. The analytical re-

Table 1

Results of the garnet-pyroxene geothermometry calculated for pressure of 20 kbar using the calibration of Nakamura (2009)

Garnet							Clinopyroxene							
Analysis	Fe	Mg	Alm	Prp	Grs	Sps	Analysis	Fe	Mg	Al	XFe	XMg	K_D	T [°C]
The intermediate granulite (Gr-pb)														
Grt core							Cpx inclusion in Grt							
Grt1aL16	1.490	0.560	0.50	0.19	0.30	0.01	Px3-1	0.178	0.319	0.591	0.163	0.294	4.78	898
Grt1aL17	1.502	0.551	0.50	0.19	0.30	0.01	Px3-2	0.180	0.332	0.573	0.166	0.306	5.02	880
Grt1aL18	1.490	0.535	0.51	0.18	0.30	0.01	Px3-3	0.182	0.331	0.579	0.167	0.303	5.05	878
													Min.	878
													Max.	898
													Ave.	885
Grt rim							Matrix Cpx							
Grt1aL02	1.468	0.682	0.49	0.23	0.27	0.01	Px1-8	0.236	0.466	0.391	0.216	0.426	4.24	915
Grt1aL03	1.453	0.681	0.49	0.23	0.27	0.01	Px1-9	0.245	0.486	0.371	0.223	0.441	4.23	916
Grt1aL04	1.461	0.674	0.50	0.23	0.27	0.01	Px1-10	0.222	0.457	0.399	0.206	0.424	4.46	895
Grt1aL05	1.481	0.658	0.50	0.22	0.27	0.01	Px1-11	0.228	0.455	0.410	0.209	0.416	4.49	894
Grt1aL06	1.468	0.646	0.50	0.22	0.27	0.01	Px2-1	0.223	0.449	0.434	0.202	0.406	4.58	890
Grt1aL07	1.491	0.656	0.50	0.22	0.27	0.01	Px2-2	0.210	0.405	0.495	0.190	0.365	4.38	911
Grt1aL08	1.484	0.637	0.50	0.21	0.28	0.01	Px2-3	0.219	0.433	0.464	0.197	0.388	4.60	893
Grt1aL09	1.491	0.624	0.50	0.21	0.28	0.01	Px2-4	0.216	0.416	0.466	0.197	0.379	4.60	894
Grt1aL10	1.482	0.610	0.50	0.21	0.28	0.01	Px2-5	0.217	0.420	0.466	0.197	0.380	4.70	889
													Min.	889
													Max.	916
													Ave.	899
The mafic granulite (GS55-1)														
Grt-Cpx pair 1														
Grt1-2	1.588	0.633	0.525	0.209	0.255	0.010	Px1-10	0.274	0.426	0.391	0.251	0.391	3.90	957
Grt1-3	1.574	0.623	0.527	0.208	0.254	0.011	Px1-10	0.274	0.426	0.391	0.251	0.391	3.93	954
Grt-Cpx pair 2														
Grt2-2	1.600	0.603	0.531	0.200	0.258	0.011	Px1-2	0.277	0.422	0.417	0.248	0.378	4.04	946
Grt2-3	1.551	0.601	0.520	0.202	0.269	0.010	Px1-3	0.282	0.421	0.403	0.255	0.381	3.84	972
Grt2-4	1.564	0.633	0.524	0.212	0.252	0.012	Px1-3	0.282	0.421	0.403	0.255	0.381	3.68	983
Grt-Cpx pair 3														
Grt2A-2	1.608	0.607	0.537	0.203	0.249	0.011	Px1-2	0.283	0.424	0.404	0.255	0.382	3.97	951
Grt2A-3	1.566	0.629	0.526	0.211	0.252	0.011	Px1-3	0.268	0.422	0.410	0.244	0.383	3.92	954
													Min.	946
													Max.	983
													Ave.	959

sults were interpreted according to the structural position and the composition of the internal domains of each monazite. Afterward, the U, Th and Pb concentrations in the monazite were recalculated using the age equations from Montel et al. (1996) and evaluated using in-house software (P. Konečný, unpublished; for more analytical details, see Konečný et al., 2004; Petrík and Konečný, 2009; Vozárová et al., 2014).

MONAZITE GEOCHRONOLOGY

The monazite forms anhedral-to-subhedral grains with sizes of 10–50 μm. The monazite grains are hosted between matrix quartz and feldspar, and certain grains are attached to garnet. Occasional monazite inclusions in garnet and allanite are also observed.

Nine matrix monazite grains, two inclusions in garnet and one inclusion in allanite were selected for analysis (Fig. 7). Forty-five analyses out of the 54 performed were used for age calculations; 9 were rejected due to questionable quality related to analytical spots in revealed cracks or over-burned spots. The average compositions of the textural populations of the matrix monazite and inclusions in garnet are similar (Table 2). The matrix monazite contains 6.62–12.48 wt.% ThO_2 (average 9.01 wt.%). 0.06–1.01 wt.% UO_2 (average 0.45 wt.%) and 0.10–0.21 wt.% PbO (average 0.15 wt.%; Table 2). The monazite grains forming inclusions in garnet contain 7.33–9.98 wt.% ThO_2 (average 8.31 wt.%). 0.16–1.04 wt.% UO_2 (average 0.74 wt.%) and 0.11–0.19 wt.% PbO (average 0.15 wt.%; Table 2). Lower concentrations of 4.44–4.79 wt.% ThO_2, 0.07–0.08 wt.% UO_2 and 0.07 wt.% PbO were determined in the monazite inclusion in allanite.

The single Th-U-total Pb dates for matrix monazite are distributed between 373 and 331 Ma, similar to the range of 359 to 331 Ma yielded by monazite inclusions in garnet (Table 3). Some matrix grains revealed Th enrichment in rims with respect

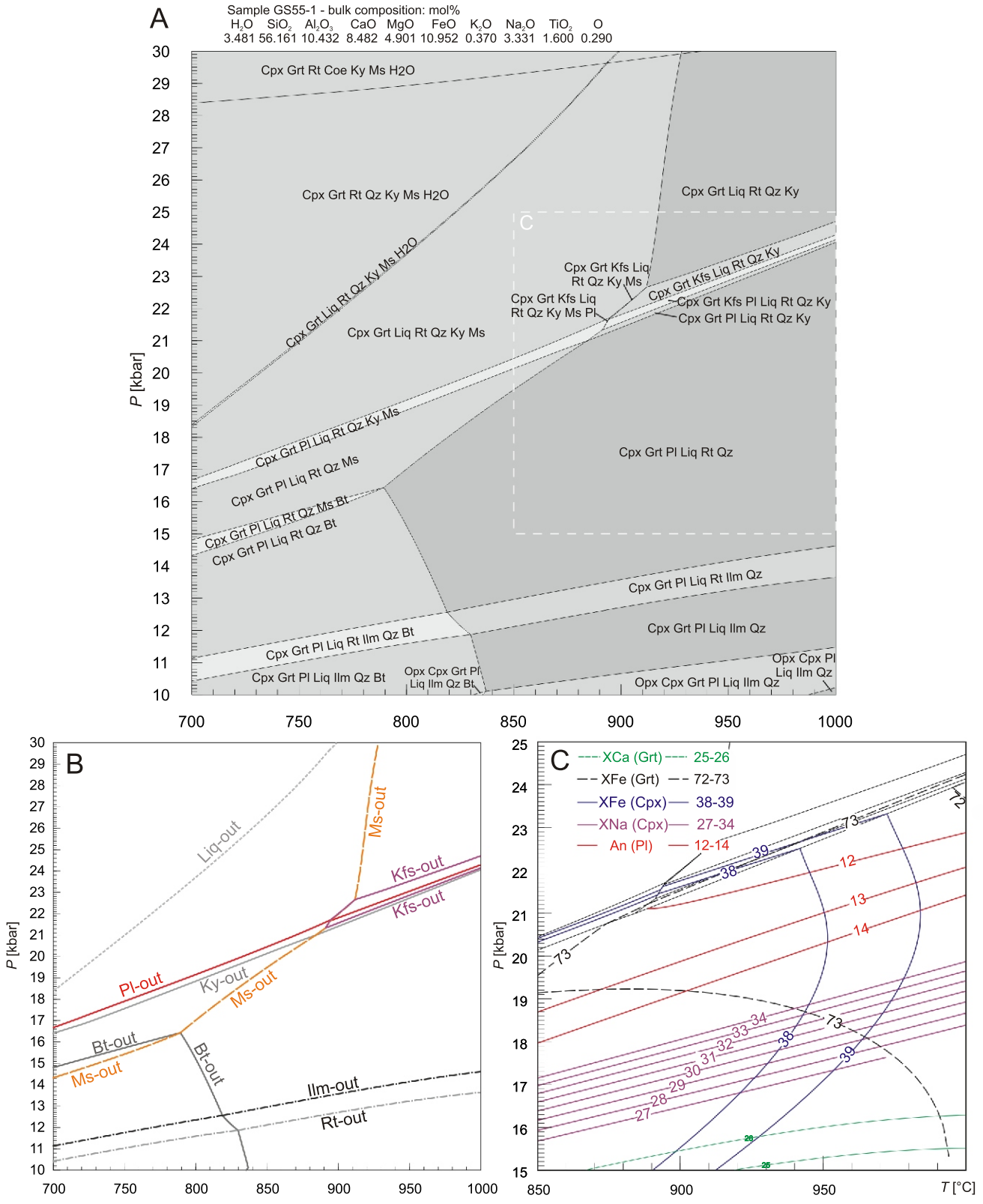

Fig. 6A – P-T pseudosection calculated for the mafic granulite rock composition (sample GS55-1); B – calculated stability of the rock-forming minerals; C – enlarged portion of the P-T pseudosection showing the calculated compositional isopleths compared to the measured composition of the garnet, plagioclase and clinopyroxene in the peak temperature mineral assemblage

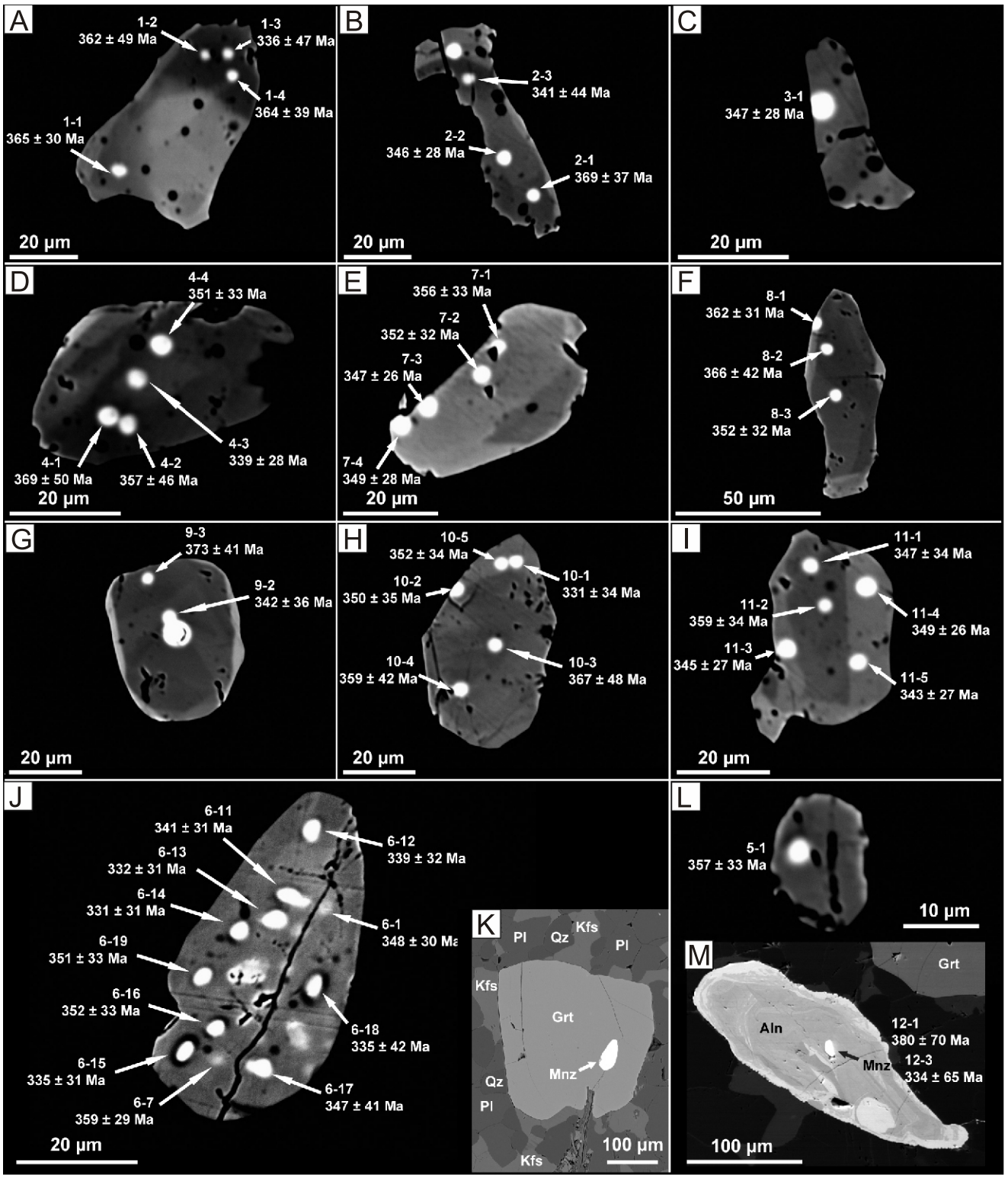

Fig. 7. The monazite grains in the intermediate granulite (sample Gr-pb) with analytical spots corresponding to the data in Tables 2 and 3

A–I – matrix monazite; **J–L** – monazite inclusions in the garnet; **M** – monazite inclusion in the allanite, BSE images; Th-U-total Pb dates are presented with ±2 error (95% confidence interval)

Table 2

Chemical composition of the matrix monazite and the monazite inclusions in the garnet and allanite in the intermediate granulite Gr-pb

	Matrix, n = 31			Inclusion in garnet, n = 12			Inclusion in allanite	
	Min.	Max.	Ave.	Min.	Max.	Ave.	12-1	12-3
P_2O_5	27.33	29.57	28.79	27.12	28.96	27.66	30.07	29.27
As_2O_5	0.11	0.15	0.13	<0.02	0.13	0.05	<0.02	<0.02
SiO_2	0.51	2.00	0.93	0.62	0.79	0.69	0.59	0.67
ThO_2	6.62	12.48	9.01	7.33	9.98	8.31	4.44	4.79
UO_2	0.06	1.01	0.45	0.16	1.04	0.74	0.08	0.07
Al_2O_3	<0.02	0.14	0.03	–	<0.02	–	<0.02	0.05
Y_2O_3	<0.03	0.15	0.06	0.05	0.12	0.09	0.03	0.05
La_2O_3	14.32	18.19	16.64	15.84	17.54	16.40	17.25	17.49
Ce_2O_3	26.14	30.69	28.64	27.39	29.72	28.37	31.39	31.37
Pr_2O_3	2.73	3.06	2.91	2.83	2.96	2.91	3.25	3.20
Nd_2O_3	8.90	10.61	9.37	9.15	10.01	9.65	10.93	10.57
Sm_2O_3	0.54	1.42	0.89	0.73	1.23	1.01	1.06	0.93
Eu_2O_3	0.08	0.25	0.16	0.10	0.24	0.18	0.09	0.09
Gd_2O_3	<0.07	0.52	0.25	0.18	0.58	0.44	0.34	0.37
Tb_2O_3	–	<0.09	–	–	<0.09	–	<0.09	<0.09
Dy_2O_3	–	<0.08	–	–	<0.08	–	<0.08	<0.08
Ho_2O_3	–	<0.10	–	–	<0.10	–	<0.10	<0.10
Er_2O_3	0.26	0.36	0.31	0.26	0.33	0.30	0.27	0.27
Tm_2O_3	<0.07	0.11	0.08	<0.07	0.10	0.08	0.08	0.12
Yb_2O_3	<0.07	0.17	0.12	<0.07	0.15	0.12	0.13	0.14
Lu_2O_3	<0.09	0.16	0.11	<0.09	0.13	0.10	<0.09	<0.09
FeO	<0.05	0.56	0.19	0.50	0.97	0.66	0.35	0.42
CaO	1.03	1.83	1.37	1.23	1.73	1.42	1.32	1.14
SrO	<0.04	0.63	0.26	0.14	0.56	0.46	0.09	0.07
PbO	0.10	0.21	0.15	0.11	0.19	0.15	0.07	0.07
SO_3	<0.02	0.17	0.04	<0.02	0.03	0.02	<0.02	<0.02
Total	99.36	102.11	100.89	98.75	100.86	99.81	101.84	101.16

to cores (Fig. 7F, H, I); however, single spot dates obtained in both of the compositional domains are within the analytical error. Only two dates were obtained from monazite inclusions in allanite, 380 ± 70 Ma and 334 ± 65 Ma, which are within the error of the other dates. The calculated weighted average age from the entire population is 349 ± 2.5 Ma (MSWD = 1.52, n = 45; Fig. 8).

DISCUSSION

PRESSURE-TEMPERATURE CONSTRAINTS

In accordance with most previously published thermobarometric data, our new P-T estimates obtained via pseudosection calculations indicate that the OSD granulites represent a deeply buried part of the Variscan Orogen (Fig. 1A). The previous geochemical data showed that the felsic and mafic granulites from the Góry Złote Mts. originated from a bimodal volcanic sequence (Bakun-Czubarow, 1998). Although the whole rock geochemistry is limited (Appendix 6), the TAS and AFM classification diagrams indicate that the protolith of the mafic granulite is related to subalkaline rocks from a tholeiitic suite, agreeing with the results of a previous study by Bakun-Czubarow (1998). The ratios of Y/Nb, Yb/Ta, (Y+Nb)/Rb and (Yb+Ta)/Rb in the felsic and intermediate granulites were compared to the discrimination diagrams in Pearce et al. (1984), and the results suggest that the protolith of the felsic and intermediate granulites is related to volcanic arc granites or within-plate granites. This detailed determination of the protoliths must be treated with caution due to the mineral reactions and likely modification of the bulk composition during high-grade progressive metamorphism. The stability fields of the assemblages related to the main granulite-facies metamorphism indicates decompression from below ultrahigh-pressure conditions to conditions exceeding 800°C and 15 kbar. The trends of the isopleths in the pseudosections do not correspond to the measured chemistry of the minerals in some cases, which makes detailed P-T constraints more difficult. However, a comparison of the mineral stability diagrams and the results from conventional thermobarometry to some extent provides information about the metamorphic history of the rocks studied. Our P-T calculations show that the protoliths of the felsic, intermediate and mafic OSD granulites were buried and experienced a main granulite-facies event at depths corresponding to 20–22 kbar and subsequently uplifted to 16–17 kbar at temperatures >900°C. These conditions were defined based on both the stability fields of the successive mineral assemblages and the preserved chemical compositions of the minerals representing the HP-HT event. Nevertheless, the possibility that the granulites experienced the ultrahigh-pressure conditions pro-

Table 3

Results of the electron microprobe analyses of the monazite in the intermediate granulite Gr-pb from Stary Gierałtów, presenting the Th, U, Pb, Y and Th* contents (in wt.%) and the calculated ages with ±2 error (95% confidence interval)

Analysis	Comment	Th	±2s	U	±2s	Pb	±2s	Y	Th*	Age [Ma]	±2s
1-1	matrix	8.363	0.074	0.679	0.014	0.173	0.006	0.032	10.58	365	30
1-2	matrix	5.952	0.056	0.066	0.012	0.100	0.006	0.003	6.17	362	49
1-3	matrix	6.022	0.057	0.072	0.012	0.094	0.006	0.019	6.26	336	47
1-4	matrix	6.831	0.063	0.310	0.013	0.128	0.006	0.018	7.84	364	39
2-1	matrix	7.202	0.066	0.382	0.013	0.139	0.006	0.038	8.45	369	37
2-2	matrix	8.676	0.077	0.901	0.015	0.179	0.006	0.036	11.61	346	28
2-3	matrix	6.478	0.060	0.103	0.012	0.104	0.006	0.026	6.81	341	44
3-1	matrix	8.863	0.078	0.821	0.015	0.179	0.006	0.033	11.54	347	28
4-1	matrix	5.822	0.055	0.071	0.012	0.100	0.006	0.014	6.05	369	50
4-2	matrix	6.330	0.059	0.067	0.012	0.105	0.006	0.006	6.55	357	46
4-3	matrix	8.900	0.078	0.867	0.015	0.178	0.006	0.044	11.72	339	28
4-4	matrix	7.586	0.068	0.589	0.014	0.149	0.006	0.047	9.50	351	33
7-1	matrix	8.125	0.072	0.496	0.013	0.155	0.006	0.115	9.74	356	33
7-2	matrix	8.159	0.073	0.503	0.013	0.154	0.006	0.103	9.80	352	32
7-3	matrix	10.777	0.092	0.609	0.014	0.198	0.006	0.093	12.76	347	26
7-4	matrix	10.966	0.094	0.213	0.012	0.182	0.006	0.031	11.66	349	28
8-1	matrix	10.054	0.087	0.086	0.012	0.168	0.006	0.018	10.34	362	31
8-2	matrix	6.816	0.063	0.163	0.012	0.120	0.006	0.037	7.35	366	42
8-3	matrix	7.330	0.067	0.804	0.014	0.156	0.006	0.086	9.95	352	32
9-2	matrix	7.898	0.071	0.179	0.012	0.130	0.006	0.035	8.48	342	36
9-3	matrix	7.114	0.065	0.119	0.012	0.125	0.006	0.048	7.50	373	41
10-1	matrix	9.027	0.079	0.071	0.012	0.147	0.006	0.013	9.26	331	34
10-2	matrix	8.647	0.076	0.078	0.012	0.139	0.006	0.017	8.90	350	35
10-3	matrix	5.867	0.056	0.129	0.012	0.103	0.006	0.017	6.29	367	48
10-4	matrix	6.804	0.063	0.148	0.012	0.117	0.006	0.020	7.28	359	42
10-5	matrix	8.964	0.079	0.080	0.012	0.145	0.006	0.012	9.22	352	34
11-1	matrix	6.186	0.058	0.905	0.015	0.141	0.006	0.098	9.13	347	34
11-2	matrix	6.186	0.058	0.895	0.015	0.146	0.006	0.097	9.10	359	34
11-3	matrix	9.505	0.083	0.794	0.015	0.186	0.006	0.105	12.09	345	27
11-4	matrix	10.060	0.087	0.785	0.015	0.197	0.006	0.108	12.62	349	26
11-5	matrix	9.849	0.085	0.764	0.014	0.189	0.006	0.099	12.34	343	27
5-1	inclusion in Grt	6.438	0.060	0.927	0.015	0.151	0.006	0.096	9.46	357	33
6-1	inclusion in Grt	8.084	0.072	0.664	0.014	0.159	0.006	0.074	10.25	348	31
6-7	inclusion in Grt	8.768	0.077	0.740	0.014	0.179	0.006	0.053	11.18	359	29
6-11	inclusion in Grt	7.481	0.068	0.764	0.015	0.152	0.006	0.074	9.97	341	31
6-12	inclusion in Grt	7.488	0.068	0.730	0.015	0.149	0.006	0.083	9.86	339	32
6-13	inclusion in Grt	7.512	0.068	0.744	0.015	0.147	0.006	0.081	9.93	332	31
6-14	inclusion in Grt	7.532	0.068	0.762	0.015	0.148	0.006	0.085	10.01	331	31
6-15	inclusion in Grt	7.198	0.065	0.791	0.015	0.146	0.006	0.074	9.77	335	31
6-16	inclusion in Grt	6.980	0.064	0.796	0.015	0.150	0.006	0.084	9.57	352	33
6-17	inclusion in Grt	6.821	0.062	0.153	0.012	0.113	0.006	0.046	7.32	347	41
6-18	inclusion in Grt	6.454	0.060	0.177	0.012	0.105	0.006	0.039	7.03	335	42
6-19	inclusion in Grt	6.851	0.063	0.785	0.015	0.147	0.006	0.075	9.41	351	33
12-1	inclusion in Aln	3.903	0.041	0.079	0.012	0.071	0.006	0.021	4.16	380	70
12-3	inclusion in Aln	4.213	0.043	0.070	0.012	0.066	0.006	0.039	4.44	334	65

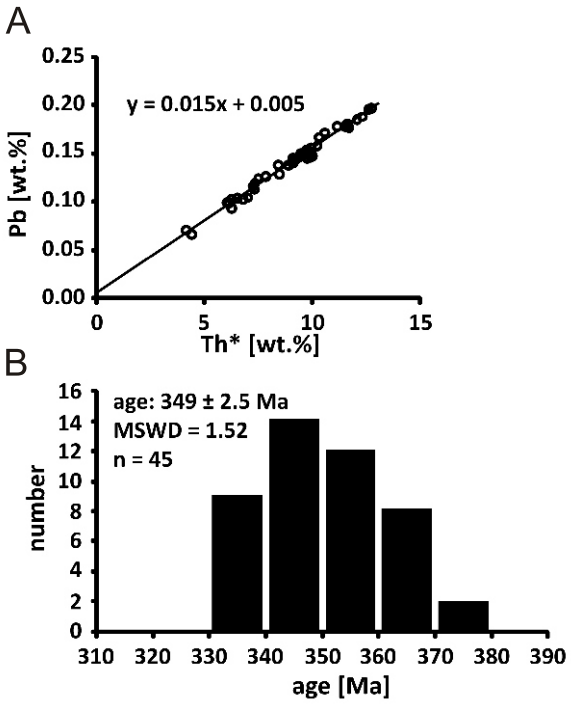

Fig. 8. Results of the Th-U-total Pb monazite geochronology in the intermediate granulite (sample Gr-pb)

Age is given with ±2 error (95% confidence interval)

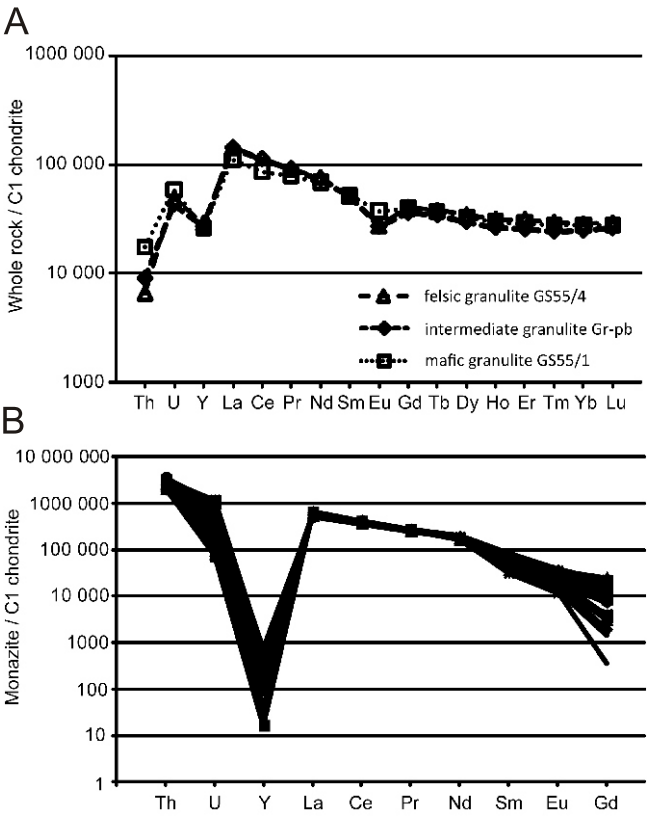

Fig. 9. C1 chondrite-normalized Th. U and REE patterns in (A) whole rocks and (B) monazite from the intermediate granulite (Gr-pb)

The chondrite values are from McDonough and Sun (1995)

posed by Bakun-Czubarow (1991b, 1992) cannot be entirely excluded because the rocks studied primarily recorded the peak temperature associated with the Variscan metamorphism and the subsequent pressure and temperature decrease. The calculations performed by both pseudosection and conventional thermometry yielded a temperature of ca. 900–920°C for the more felsic granulites and ca. 950–970°C for the mafic granulites. Our data reveal good agreement with the previous calculations of Kryza et al. (1996), who reported pressures of 22 and 25 kbar at 800–900°C, and Štípská et al. (2004), who reported conditions of 18–19 kbar at ca. 900°C.

The granulite body exposed in the Góry Złote Mts. recorded vertical extrusion to middle crustal depths (Štípská et al., 2004). Our study indicates that the decompresion is evidenced by the development of Cpx symplectites in the more mafic granulites and the formation of subordinate ilmenite and biotite in all studied samples, which developed under conditions of less than 13–14 kbar and ca. 850°C. The HP-HT conditions reported in the OSD granulites and eclogites (review in Żelaźniewicz et al., 2014) contrast with the medium-grade, primarily amphibolite-facies conditions of the metasedimentary rocks (review in Chopin et al., 2012; Jastrzębski et al., 2015a). The Orlica–Śnieżnik Dome is thus composed of both HP-HT and medium-grade rocks that share only a portion of their tectonometamorphic evolution (e.g., Štípská et al., 2004, 2012; Skrzypek et al., 2011).

INTERPRETATION OF THE MONAZITE Th-U-total Pb AGES

The similar composition of the two textural populations of monazite, the matrix grains and the inclusions in garnets, indicates that both formed with the same available chemical budget. There is no high Y content in monazite, including the monazite inclusions shielded by garnet with respect to the matrix monazite, that could suggest that the monazite formed prior to garnet, which incorporates the available yttrium. The low Y concentrations in all monazite grains (Table 3 and Fig. 9B), which are also reflected by the limited Y budget in the whole rock composition (Fig. 9A), indicate that monazite growth occurred after the initial growth of garnet. Lack of pronounced negative anomalies of Eu at the chondrite-normalized plot (Fig. 9B) and slight enrichment in Sr (up to 0.63 wt.% SrO; Table 2) suggest monazite growth occurred after plagioclase breakdown related to the reactions of garnet and clinopyroxene formation or before formation of the plagioclase during retrogression. These observations are indicative of monazite growth during progressive metamorphism, probably during an HP-HT stage. Regarding monazite shielded by allanite, interpreted as related to the magmatic protolith, there is no clear evidence to define its origin (Fig. 7M). The textural setting of monazite and different composition with respect to other textural populations of monazite (Table 2) suggest that its origin is related to crystallisation in the granitic protolith of the granulite.

The 349 ± 2.5 Ma age of the monazite from this study is similar to the previously reported 347 ± 13 Ma monazite Th-U-total Pb age from a felsic granulite (Kusiak et al., 2008), but our result is more tightly constrained. Previous work reported a wide range of Th-U-total Pb single dates from 278 to 411 Ma, most likely due to lower analytical precision. Kusiak et al. (2008) bolstered their results with garnet ages from Anczkiewicz et al. (2007) and interpreted the age of ca. 347 Ma as the timing of amphibolite facies metamorphism during retrogression from (U)HP conditions. The origin of the scattered dates was ex-

plained by these authors as the result of resorption due to monazite-consuming reactions or analytical error.

In the present paper, the textural context of monazite, the complete analysis of other elements required to control the monazite composition, and the eventual rejection of analyses with questionable quality were considered. The Th-U-total Pb dates yielded by all textural populations of the monazite (matrix grains, inclusions in garnet, and inclusions in allanite) indicate a single metamorphic episode with the metamorphic peak constrained to 349 ± 2.5 Ma. Because the closure temperature of the volume diffusion of Pb in monazite is 800–900°C (Cherniak et al., 2004; Gardes et al., 2006; Cherniak and Pyle, 2008), monazite likely experienced Pb diffusion during the HP-HT metamorphic stage at 900–970°C. This indicates that the obtained age presumably does not reflect the timing of subduction; rather, it reflects the onset of cooling and decompression under relatively high-temperature conditions (Fig. 5). Earlier monazite geochronometry studies indicated the possibility of ca. 380–370 Ma progressive metamorphism in the region, although primarily based on medium-grade rocks (Gordon et al., 2005; Jastrzębski et al., 2013, 2014, 2015a). There is no evidence that the monazite preserved older ages related to growth during processes that occurred earlier than ca. 349 Ma, such as, for instance, those observed in zircon (Bröcker et al., 2010). Our geochronology data are, however, in agreement with the ca. 341 and 342 Ma zircon ages provided by Štípská et al. (2004). The zircon U-Pb dating of the HT metamorphic processes is also limited to the closure temperature of the U-Th-Pb isotopic system, which is estimated to be >900°C (Lee et al., 1997; Cherniak and Watson, 2001). Consequently, the zircon U-Pb ages recorded prior to the (U)HP-HT stage of the OSD granulites were disturbed by the 900–1000°C metamorphic conditions (cf. Bröcker et al., 2010). The late stage of the (U)HP-HT metamorphism resulted in the alteration of the zircon from the protolith and the growth of metamorphic zircon in the granulites and eclogites at 350–330 Ma (Bröcker et al., 2010). The youngest zircon age, 326 ± 2 Ma, was attributed to the cooling path from amphibolite to greenschist facies (Lange et al., 2005). Recent monazite geochronology indicates that dates clustering around 290 Ma are characteristic for rocks of the Sudetic part of Brunovistulia (Schulmann et al., 2014). Nevertheless, our monazite data show that there are no monazite overgrowths or textures indicative of metamorphic overprint in the OSD granulites during retrogression. Additionally, no evidence exists for fluid-mediated alterations post-dating the HP-HT stage that might have led to the disturbance of the Th-U-Pb system via a fluid-aided coupled dissolution-reprecipitation process, even during relatively low-temperature processes (cf. Williams et al., 2011; Budzyń et al., 2015). Consequently, the 349 ± 2.5 Ma age for the monazite is interpreted here as being related to a late-stage of HP-HT metamorphism and the beginning of cooling below 900°C.

A significantly older Lu-Hf garnet age of 380–370 Ma reported by Anczkiewicz et al. (2007) is unique amongst studies involving geochronology in the granulites from Stary Gierałtów. In a later work, Walczak (2011) applied the same analytical methods as Anczkiewicz et al. (2007) and obtained Lu-Hf ages of 350–340 Ma. The discrepancy in the results was explained by Walczak (2011) as most likely related to the dissolution of Hf-bearing phases in the whole rock fraction, such as metamict zircon, that could modify the whole rock (WR) Lu/Hf ratios and resulted in the older Lu-Hf Grt-WR isochron ages presented by Anczkiewicz et al. (2007). Because the closure temperatures of 700 ± 50°C for Sm-Nd (Ganguly et al., 1998) and >750°C for Lu-Hf systems in garnet (Scherer et al., 2000) are lower than that of the Th-U-Pb system in monazite, the current monazite in situ geochronology agrees better with most of the previous garnet-dating results (Brueckner et al., 1991; Lange et al., 2005; Walczak, 2011).

CONCLUSIONS

The current thermodynamic modelling indicates that the felsic and mafic granulites from the OSD experienced comparable P-T granulite-facies conditions: ca. 20–22 kbar and ca. 900–920°C with a ca. 4–6 kbar isothermal pressure decrease for more felsic granulites and ca. 18–20 kbar and ca. 950–970°C for the more mafic granulite. The new geochronological data constrain the Th-U-total Pb age of monazite to 349 ± 2.5 Ma for the late stage of the HP-HT metamorphic stage. The age corresponds to the initial exhumation of the granulites and cooling below temperatures of ca. 900°C. The comparison of the P-T-t record of the granulites from the Góry Złote Mts. with the P-T-d-t data published from the OSD indicates that the channels that exhumed the HP rocks to mid-crustal depths were active at ca. 350 Ma and that from ca. 340 Ma onward, all types of metamorphic rocks from the OSD presumably shared a common Variscan evolution. The high-temperature conditions (above the closure temperatures of the isotopic systems used in geochronology) prevented the HP-HT granulites and eclogites from recording the supposed earlier, syn-collisional Late Devonian metamorphism evidenced in the region.

Acknowledgements. This work was funded by the National Science Centre of Poland, grant number DEC 2011/03/B/ST10/05638. L. Jeżak, P. Dzierżanowski, I. Holický and V. Kollárová are acknowledged for their assistance during the electron microprobe analyses. W. Stawikowski is greatly acknowledged for discussions during field work. The article greatly benefited from reviews by I. Petrík, P. Štípská and an anonymous reviewer, and from editorial handling by T. Peryt.

REFERENCES

Anczkiewicz, R., Szczepański, J., Mazur, S., Storey, C., Crowley, Q., Villa, I.M., Thirlwall, M.F., Jeffries, T.E., 2007. Lu-Hf geochronology and trace element distribution in garnet: Implications for uplift and exhumation of ultra-high pressure granulites in the Sudetes, SW Poland. Lithos, **95**: 363–380.

Bakun-Czubarow, N., 1991a. Geodynamic significance of the Variscan high-P eclogite-granulite series of the Złote Mountains in the Sudetes. Publications of Institute of Geophysics, Polish Academy of Sciences, A19, **236**: 215–244.

Bakun-Czubarow, N., 1991b. On the possibility of occurrence of quartz pseudomophs after coesite in the eclogite-granulite rock

series of the Złote Mountains in the Sudetes (SW Poland). Archiwum Mineralogiczne, **47**: 5–16.

Bakun-Czubarow, N., 1992. Quartz pseudomorphs after coesite and quartz exsolutions in eclogitic clinopyroxenes of the Złote Mountains in the Sudetes (SW Poland). Archiwum Mineralogiczne, **48**: 3–25.

Bakun-Czubarow, N., 1998. Ilmenite-bearing eclogites of the West Sudetes – their geochemistry and mineral chemistry. Archiwum Mineralogiczne, **51**: 29–110.

Bröcker, M., Klemd, R., Kooijman, E., Berndt, J., Larionov, A., 2010. Zircon geochronology and trace element characteristics of eclogites and granulites from the Orlica-Śnieżnik complex, Bohemian Massif. Geological Magazine, **147**: 339–362.

Brueckner, H.K., Medaris, L.G., Bakun-Czubarow, N., 1991. Nd and Sr age and isotope patterns from Variscan eclogites of the eastern Bohemian Massif. Neues Jahrbuch für Mineralogie, Abhandlungen, **163**: 169–196.

Budzyń, B., Konečný, P., Kozub-Budzyń, G.A., 2015. Stability of monazite and disturbance of the Th-U-Pb system under experimental conditions of 250–350°C and 200–400 MPa. Annales Societatis Geologorum Poloniae, **85**: 405–424.

Chopin, F., Schulmann, K., Skrzypek, E., Lehmann, J., Dujardin, J.R., Martelat, J.E., Lexa, O., Corsini, M., Edel, J.B., Štípská, P., Pitra, P., 2012. Crustal influx, indentation, ductile thinning and gravity redistribution in a continental wedge: building a Moldanubian mantled gneiss dome with underthrust Saxothuringian material (European Variscan belt). Tectonics, **31**: TC1013.

Cherniak, D.J., Pyle, J.M., 2008. Th diffusion in monazite. Chemical Geology, **256**: 52–61.

Cherniak, D.J., Watson, E.B., 2001. Pb diffusion in zircon. Chemical Geology, **172**: 5–24.

Cherniak, D.J., Watson, E.B., Grove, M., Harrison, T.M., 2004. Pb diffusion in monazite: a combined RBS/SIMS study. Geochimica et Cosmochimica Acta, **68**: 829–840.

Coggon, R., Holland, T.J.B., 2002. Mixing properties of phengitic micas and revised garnet-phengite thermobarometers. Journal of Metamorphic Geology, **20**: 683–696.

Cymerman, Z., Piasecki, M.A.J., Seston, R., 1997. Terranes and terrane boundaries in the Sudetes, Northeast Bohemian Massif. Geological Magazine, **134**: 717–725.

Don, J., Dumicz, M., Wojciechowska, I., Żelaźniewicz, A., 1990. Lithology and tectonics of the Orlica-Śnieżnik Dome, Sudetes - recent state of knowledge. Neues Jahrbuch für Geologie und Paläontologie Abhandlungen, **197**: 159–188.

Don, J., Skácel, J., Gotowała, R., 2003. The boundary zone of the East and West Sudetes on the 1:50 000 scale geological map of the Velké Vrbno, Staré Město and Śnieżnik Metamorphic Units. Geologia Sudetica, **35**: 25–59.

Dumicz, M., 1993. The history of eclogites in the geological evolution of the Śnieżnik crystalline complex based on mesostructural analysis. Geologia Sudetica, **27**: 21–64.

Ferrero, S., Wunder, B., Walczak, K., O´Brien, P.J., Ziemann, M.A., 2015. Preserved near ultrahigh-pressure melt from continental crust subducted to mantle depths. Geology, **43**: 447–450.

Franke, W., Żelaźniewicz, A., 2000. The eastern termination of the Variscides: terrane correlation and kinematic evolution. Geological Society Special Publications, **179**: 63–86.

Ganguly, J., Tirone, M., Hervig, R.L., 1998. Diffusion kinetics of samarium and neodymium in garnet, and a method for determining cooling rates of rocks. Science, **281**: 805–807.

Gardes, E., Jaoul, O., Montel, J., Seydoux-Guillaume, A.M., Wirth, R., 2006. Pb diffusion in monazite: an experimental study of Pb^{2+} + Th^{4+} – $2Nd^{3+}$ interdiffusion. Geochimica et Cosmochimica Acta, **70**: 2325–2336.

Gordon, S.M., Schneider, D.A., Manecki, M., Holm, D.K., 2005. Exhumation and metamorphism of an ultrahigh-grade terrane: geochronometric investigations of the Sudetes Mountains (Bohemia), Poland and Czech Republic. Journal of the Geological Society, **162**: 841–855.

Green, E.C.R., Holland, T.J.B,, Powell, R. 2007. An order-disorder model for omphacitic pyroxenes in the system jadeite-diopside-hedenbergite-acmite, with applications to eclogite rocks. American Mineralogist, **92**: 1181–1189.

Holland, T.J.B., Powell, R., 1998. An internally consistent thermodynamic data set for phases of petrological interest. Journal of Metamorphic Geology, **16**: 309–343.

Holland, T.J.B., Powell, R., 2003. Activity-composition relations for phases in petrological calculations: an asymmetric multicomponent formulation. Contributions to Mineralogy and Petrology, **145**: 492–501.

Jastrzębski, M., Żelaźniewicz, A., Majka, J., Murtezi, M., Bazarnik, J., Kapitonov, I., 2013. Constraints on the Devonian–Carboniferous closure of the Rheic Ocean from a multi-method geochronology study of the Staré Město Belt in the Sudetes (Poland and the Czech Republic). Lithos, **170–171**: 54–72.

Jastrzębski, M., Stawikowski, W., Budzyń, B., Orłowski, R., 2014. Migmatization and large-scale folding in the Orlica-Śnieżnik Dome, NE Bohemian Massif: Pressure-temperature-time-deformation constraints on Variscan terrane assembly. Tectonophysics, **630**: 54–74.

Jastrzębski, M., Budzyń, B., Stawikowski, W., 2015a. Structural, metamorphic and geochronological record in the Goszów quartzites of the Orlica-Śnieżnik Dome (SW Poland): implications for the polyphase Variscan tectonometamorphism of the Saxothuringian Terrane. Geological Journal, doi: 10.1002/gj.2647

Jastrzębski, M., Żelaźniewicz, A., Murtezi, M., Sergeev, S., Larionov, A.N., 2015b. The Moldanubian Thrust Zone – a terrane boundary in the Central European Variscides refined based on lithostratigraphy and U-Pb zircon geochronology. Lithos, **220–223**: 116–132.

Kądziałko-Hofmokl, M., Szczepański, J., Werner, T., Jeleńska, M., Nejbert, K. 2013. Paleomagnetism and magnetic mineralogy of metabasites and granulites from Orlica-Śnieżnik Dome (Central Sudetes). Acta Geophysica, **61**: 535–568.

Kelsey, D.E., Hand, M., 2015. On ultrahigh temperature crustal metamorphism: Phase equilibria, trace element thermometry, bulk composition, heat sources, timescales and tectonic settings. Geoscience Frontiers, **6**: 311–356.

Klemd, R., Bröcker, M., 1999. Fluid influence on mineral reactions in ultrahigh-pressure granulites: a case study in the Śnieżnik Mts. (West Sudetes, Poland). Contributions to Mineralogy and Petrology, **135**: 358–373.

Konečný, P., Siman, P., Holický, I., Janák, M., Kollárová, V., 2004. Method of monazite dating by means of the electron microprobe (in Slovak with English abstract). Mineralia Slovaca, **36**: 225–235.

Kozłowski, K., 1965. The granulitic complex of Stary Gierałtów – East Sudetes. Archiwum Mineralogiczne, **25**: 5–122.

Kryza, R., Pin, C., Vielzeuf, D., 1996. High-pressure granulites from the Sudetes (south-west Poland): evidence of crustal subduction and collisional thickening in the Variscan Belt. Journal of Metamorphic Geology, **14**: 531–546.

Kusiak, M.A., Suzuki, K., Dunkley, D.J., Lekki, J., Bakun-Czubarow, N., Paszkowski, M., Budzyń, B., 2008. EPMA and PIXE dating of monazite In granulites from Stary Gierałtów, NE Bohemian Massif, Poland. Gondwana Research, **14**: 674–685.

Lange, U., Bröcker, M., Armstrong, R., Trapp, E., Mezger, K., 2005. Sm-Nd and U-Pb dating of high-pressure granulites from the Złote and Rychleby Mts (Bohemian Massif, Poland and Czech Republic). Journal of Metamorphic Geology, **23**: 133–145.

Lee, J.K.W., Williams, I.S., Ellis, D.J., 1997. Pb, U and Th diffusion in natural zircon. Nature, **390**: 159–162.

Matte, P., Maluski, H., Rajlich, P., Franke, W., 1990. Terrane boundaries in the Bohemian Massif: result of large-scale Variscan shearing. Tectonophysics, **177**: 151–170.

Mazur, S., Aleksandrowski, P., Kryza, R., Oberc-Dziedzic, T., 2006. The Variscan Orogen in Poland. Geological Quarterly, **50** (1): 89–118.

McDonough, W.F., Sun, S.-S., 1995. The composition of the Earth. Chemical Geology, **120**: 223–253.

Montel, J.M., Foret, S., Veschambre, M., Nicollet, C., Provost, A., 1996. Electron microprobe dating of monazite. Chemical Geology, **131**: 37–53.

Nakamura, D., 2009. A new formulation of garnet–clinopyroxene geothermometer based on accumulation and statistical analysis of a large experimental data set. Journal of Metamorphic Geology, **27**: 495–508.

Pearce, J.A., Harris, N.B.W., Tindle, A.G., 1984. Trace element discrimination diagrams for the tectonic interpretation of granitic rocks. Journal of Petrology, **25**: 956–983.

Petrík, I., Konečný, P., 2009. Metasomatic replacement of inherited metamorphic monazite in a biotite-garnet granite from the Nízke Tatry Mountains, Western Carpathians, Slovakia: Chemical dating and evidence for disequilibrium melting. American Mineralogist, **94**: 957–974.

Pouba, Z., Paděra, K., Fiala, J., 1985. Omphacite granulite from the NE marginal area of the Bohemian Massif (Rychleby Mts). Neues Jahrbuch für Mineralogie Abhandlungen, **151**: 29–52.

Redlińska-Marczyńska, A., Żelaźniewicz A., 2011. Gneisses in the Orlica-Śnieżnik Dome, West Sudetes: a single batholitic protolith or a more complex origin? Acta Geologica Polonica, **61:** 307–339.

Sawicki, L., 1995. Geological Map of Lower Silesia with adjacent Czech and German Territories 1:100 000. Państwowy Instytut Geologiczny. Warszawa.

Scherer, E.E., Kenneth, C.L., Blichert-Toft, J., 2000. Lu-Hf garnet geochronology: Closure temperature relative to the Sm-Nd system and the effects of trace mineral inclusions. Geochimica et Cosmochimica Acta, **64**: 3413–3432.

Schulmann, K., Gayer, R., 2000. A model of an obliquely developed continental accretionary wedge: NE Bohemian Massif. Journal of the Geological Society, **156**: 401–416.

Schulmann, K., Lexa, O., Štípská, P., Racek, M., Tajčmanová, L., Konopásek, J., Edel., J.-B., Peschler, A., Lehmann, J., 2008. Vertical extrusion and horizontal channel flow of orogenic lower crust: key exhumation mechanisms in large hot orogens? Journal of Metamorphic Geology, **26**: 273–297.

Schulmann, K., Oliot, E., Košuličová, M., Montigny, R., Štípská, P., 2014. Variscan thermal overprints exemplified by U-Th-Pb monazite and K-Ar muscovite and biotite dating at the eastern margin of the Bohemian Massif (East Sudetes, Czech Republic). Journal of Geosciences, **59**: 389–413.

Skrzypek, E., Štípská, P., Schulmann, K., Lexa, O., Lexová, M., 2011. Prograde and retrograde metamorphic fabrics – a key for understanding burial and exhumation in orogens (Bohemian Massif). Journal of Metamorphic Geology, **29**: 451–472.

Smulikowski, K., 1967. Eclogites of the Śnieżnik Mountains in the Sudetes. Geologia Sudetica, **3**: 157–174.

Smulikowski, K., 1979. Polymetamorphic evolution of the crystalline complex of Śnieżnik and Góry Złote Mts in the Sudetes. Geologia Sudetica, **14**: 7–76.

Smulikowski, K., Bakun-Czubarow, N., 1973. New data concerning the granulite-eclogite rock series of Stary Gierałtów, East Sudetes, Poland. Bulletin de l'Academie Polonaise des Sciences, **21**: 25–34.

Szczepański, J., Anczkiewicz, R., Mazur, S., 2008. Gierałtów granulites – a vestige of an early Variscan ultra-high pressure metamorphism in the Orlica-Śnieżnik Massif, West Sudetes. Mineralogia – Special Papers, **32**: 155.

Štípská, P., Schulmann, K., Kröner, A., 2004. Vertical extrusion and middle crustal spreading of omphacite granulite: a model of syn-convergent exhumation (Bohemian Massif, Czech Republic). Journal of Metamorphic Geology, **22**: 179–198.

Štípská, P., Chopin, F., Skrzypek, E., Schulmann, K., Pitra, P., Lexa, O., Martelat, J.E., Bollinger, C., Žáčková, E., 2012. The juxtaposition of eclogite and mid-crustal rocks in the Orlica–Śnieżnik Dome, Bohemian Massif. Journal of Metamorphic Geology, **30**: 213–234.

Vozárová, A., Konečný, P., Šarinová, K., Vozár, J., 2014. Ordovician and Cretaceous tectonothermal history of the Southern Gemericum Unit from microprobe monazite geochronology (Western Carpathians, Slovakia). International Journal of Earth Sciences, **103**: 1005–1022.

Walczak, K., 2011. Interpretacja datowań Sm-Nd i Lu-Hf granatów w skałach wysokociśnieniowych i wysokotemperaturowych w świetle badań dystrybucji pierwiastków śladowych (in Polish). Unpublished Ph.D. thesis. Institute of Geological Sciences, Polish Academy of Sciences, Kraków.

White, R.W., Powell, R., Holland, T.J.B., Worley, B.A., 2000. The effect of TiO_2 and Fe_2O_3 on metapelitic assemblages at greenschist and amphibolite facies conditions: mineral equilibria calculations in the system K_2O-FeO-MgO-Al_2O_3-SiO_2-H_2O-TiO_2-Fe_2O_3. Journal of Metamorphic Geology, **18**: 497–511.

White, R.W., Powell, R., Holland, T.J.B., 2007. Progress relating to calculation of partial melting equilibria for metapelites. Journal of Metamorphic Geology, **25**: 511–527.

Whitney, D.L., Evans, B.W., 2010. Abbreviations for names of rock-forming minerals. American Mineralogist, **95**: 185–187.

Williams, M.L., Jercinovic, M.J., 2002. Microprobe monazite geochronology: putting absolute time into microstructural analyses. Journal of Structural Geology, **24**: 1013–1028.

Williams, M.L., Jercinovic, M.J., Hetherington, C.J., 2007. Microprobe monazite geochronology: understanding geologic processes by integrating composition and chronology. Annual Review of Earth and Planetary Sciences, **35**: 137–175.

Williams, M.L., Jercinovic, M.J., Harlov, D.E., Budzyń, B., Hetherington, C.J., 2011. Resetting monazite ages during fluid-related alteration. Chemical Geology, **283**: 218–225.

Żelaźniewicz, A., Jastrzębski, M., Redlińska-Marczyńska, A., Szczepański, J., 2014. The Orlica–Śnieżnik Dome, the Sudetes, in 2002 and 12 years later. Geologia Sudetica, **42**: 105–123.